BBA - Molecular Basis of Disease 1865 (2019) 2224–2245

Contents lists available at ScienceDirect

BBA - Molecular Basis of Disease

journal homepage: www.elsevier.com/locate/bbadis

Astaxanthin exerts protective effects similar to bexarotene in Alzheimer's disease by modulating amyloid-beta and cholesterol homeostasis in blood-brain barrier endothelial cells

Elham Fanaee-Danesh[a], Chaitanya Chakravarthi Gali[a], Jelena Tadic[b], Martina Zandl-Lang[a], Alexandra Carmen Kober[a], Vicente Roca Agujetas[c], Cristina de Dios[c,d], Carmen Tam-Amersdorfer[a], Anika Stracke[a], Nicole Maria Albrecher[a], Anil Paul Chirackal Manavalan[a], Marielies Reiter[a], Yidan Sun[a], Anna Colell[c], Frank Madeo[b,e], Ernst Malle[f], Ute Panzenboeck[a,*]

[a] Division of Immunology and Pathophysiology, Otto Loewi Research Center, Medical University of Graz, Graz, Austria
[b] Institute of Molecular Biosciences, University of Graz, Graz, Austria
[c] Department of Cell Death and Proliferation, Institut d'Investigacions Biomèdiques de Barcelona, Consejo Superior de Investigaciones Científicas (CSIC), IDIBAPS, Centro de Investigación Biomédica en Red sobre Enfermedades Neurodegenerativas (CIBERNED), Barcelona, Spain
[d] Department of Biomedicine, Facultat de Medicina, Universitat de Barcelona, Barcelona, Spain
[e] BioTechMed Graz, Graz, Austria
[f] Division of Molecular Biology and Biochemistry, Gottfried Schatz Research Center, Medical University of Graz, Graz, Austria

ARTICLE INFO

Keywords:
Blood-brain barrier
Alzheimer's disease
APP processing
ABCA1
Cholesterol efflux
LRP-1

ABSTRACT

The pathogenesis of Alzheimer's disease (AD) is characterized by overproduction, impaired clearance, and deposition of amyloid-β peptides (Aβ) and connected to cholesterol homeostasis. Since the blood-brain barrier (BBB) is involved in these processes, we investigated effects of the retinoid X receptor agonist, bexarotene (Bex), and the peroxisome proliferator-activated receptor α agonist and antioxidant, astaxanthin (Asx), on pathways of cellular cholesterol metabolism, amyloid precursor protein processing/Aβ production and transfer at the BBB in vitro using primary porcine brain capillary endothelial cells (pBCEC), and in 3xTg AD mice. Asx/Bex downregulated transcription/activity of amyloidogenic *BACE1* and reduced Aβ oligomers and ~80 kDa intracellular 6E10-reactive APP/Aβ species, while upregulating non-amyloidogenic *ADAM10* and soluble (s)APPα production in pBCEC. Asx/Bex enhanced Aβ clearance to the apical/plasma compartment of the in vitro BBB model. Asx/Bex increased expression levels of *ABCA1*, *LRP1*, and/or APOA-I. Asx/Bex promoted cholesterol efflux, partly via PPARα/RXR activation, while cholesterol biosynthesis/esterification was suppressed. Silencing of LRP-1 or inhibition of ABCA1 by probucol reversed Asx/Bex-mediated effects on levels of APP/Aβ species in pBCEC. Murine (m)BCEC isolated from 3xTg AD mice treated with Bex revealed elevated expression of *APOE* and *ABCA1*. Asx/Bex reduced *BACE1* and increased *LRP-1* expression in mBCEC from 3xTg AD mice when compared to vehicle-treated or non-Tg treated mice. In parallel, Asx/Bex reduced levels of Aβ oligomers in mBCEC and Aβ species in

Abbreviations: ABCA1, ATP binding cassette transporter subfamily A member 1; ABCG1, ATP binding cassette transporter subfamily G member 1; AD, Alzheimer's disease; Aβ, amyloid-beta peptide; APP, amyloid precursor protein; ADAM10, A disintegrin and metalloproteinase domain-containing protein 10; apoA-I, apolipoprotein A-I; apoE, apolipoprotein E; Asx, Astaxanthin; BACE1, β-site of APP cleaving enzyme, beta-secretase; BBB, blood-brain barrier; BCEC, brain capillary endothelial cells; Bex, bexarotene; CD31, cluster of differentiation 31; CD13, aminopeptidase N; CTFs, C-terminal fragments; GFAP, glial fibrillary acidic protein; GW 6471, *N*-((2*S*)-2-(((1Z)-1-Methyl-3-oxo-3-(4-(trifluoromethyl)phenyl)prop-1-enyl)amino)-3-(4-(2-(5-methyl-2-phenyl-1,3-oxazol-4-yl)ethoxy)phenyl)propyl)propanamide; HDL_3, high-density lipoprotein subclass 3; IBA1, ionized calcium binding adaptor molecule 1; LRP-1, low-density lipoprotein receptor-related protein 1; LXR, liver X receptor; mBCEC, murine BCEC; PA 452, 2-[[3-(Hexyloxy)-5,6,7,8-tetrahydro-5,5,8,8-tetramethyl-2 naphthalenyl]methylamino]-5-pyrimidinecarboxylic acid; pBCEC, porcine BCEC; PDGFRβ, beta-type platelet-derived growth factor receptor; PPAR, peroxisome proliferator-activated receptor; ROS, reactive oxygen species; RXR, retinoid X receptor; sAPPα, soluble amyloid precursor protein-α; SMA, smooth muscle actin; SYP, synaptophysin; TEER, transendothelial electrical resistance; vWF, von Willebrand factor; 3xTg AD, APP $_{Swe}$/MAPT $_{P301L}$/PSEN1 $_{M146V}$

* Corresponding author at: Division of Immunology and Pathophysiology, Otto Loewi Research Center, Medical University of Graz, Heinrichstrasse 31a, 8010 Graz, Austria.
E-mail address: ute.panzenboeck@medunigraz.at (U. Panzenboeck).

https://doi.org/10.1016/j.bbadis.2019.04.019
Received 20 November 2018; Received in revised form 28 April 2019; Accepted 30 April 2019
Available online 02 May 2019
0925-4439/

brain soluble and insoluble fractions of 3xTg AD mice. Our results suggest that both agonists exert beneficial effects at the BBB by balancing cholesterol homeostasis and enhancing clearance of Aβ from cerebrovascular endothelial cells.

1. Introduction

Alzheimer's disease (AD), a general term for short-term and gradual long-term memory loss [1], is the most common form of dementia. Different mechanisms involved in AD pathogenesis were reported [2]. Amyloid-β peptides (Aβ), the main component of plaques [3], and tangles formed by hyper phosphorylated tau (p-tau) [4], represent the two long reported cerebral hallmarks in the pathology of AD. Cerebral Aβ is normally removed via active transport across the blood-brain barrier (BBB), a process in which endothelial low-density lipoprotein receptor-related protein 1 (LRP-1) is centrally involved [5,6]. The BBB also provides protection against entry of neurotoxic compounds from the circulation. Thus, transporters in cerebrovascular endothelial cells mediate the control of cerebral Aβ levels and drug penetration into the brain [7].

When Aβ metabolism and clearance is imbalanced, Aβ deposition in mostly small arteries and arterioles causes cerebral amyloid angiopathy, occurring in AD with a frequency of 80–90% [8]. BBB dysfunction, including loss of vascular density, decreased diameter of capillaries, and impaired clearance of cerebral Aβ across the BBB may consequently contribute to AD pathogenesis [9]. Therefore, maintenance of BBB integrity is crucial to prevent AD and other neurological disorders.

The generation of Aβ can be reduced by the disintegrin and metalloproteinase domain-containing protein 10 (ADAM 10) or α-secretase, responsible for the non-amyloidogenic processing of amyloid precursor protein (APP), thereby preventing and/or improving the pathologic impairment in AD [10]. Cleavage by α-secretase occurs within the Aβ domain of APP to release the soluble, secreted 100 KDa fragment termed sAPPα [11]. Another and currently most promising strategy to prevent Aβ production appears to be inhibition of the protease β-site APP-cleaving enzyme 1 (BACE1). BACE1 catalyses the first and rate-limiting step in the amyloidogenic processing of APP [12] and was found to be elevated in brains of AD patients [13]. In humans and in animal models, Aβ production was reduced after administration of BACE1 inhibitors [14,15]. Aβ deposition could be reversed, and cognitive decline was improved upon BACE1 deletion in mice [16]. These data suggest that BACE1 represents a major drug target for AD treatment [17,18].

Interestingly, cholesterol metabolism is perturbed already in the early stages of the neurodegenerative process [19]. Increased levels of plasma cholesterol [20] and decreased levels of high-density lipoproteins (HDL) and apoA-I (the major apolipoprotein of HDL) correlate with the severity of AD [21]. Lipid transport and cholesterol homeostasis in the central nervous system (CNS) are mediated through apoA-I and apoE on HDL [22]. Lipidation of both apolipoproteins occurs by the cholesterol transporter ATP-binding cassette transporter A1 (ABCA1) [23,24]. Interestingly, memory deficits mediated through Aβ oligomers deposited in the hippocampus in aged APP23 mice were reported to be ABCA1-dependent [25]. Further, Aβ elimination from the brain was shown to be facilitated by ABCA1, which neutralized Aβ aggregation capacity in an apoE-dependent manner [26]. Lipidated apoE has been shown to adjust its Aβ-binding and consequently degradation properties [27], and the accumulation of Aβ in the brain was reported in cholesterol-fed animal models [28]. Aβ itself may induce membrane-associated oxidative stress [29], and exposure of brain cells to oxidative stress causes cholesterol accumulation in cellular membranes [30]. A regulatory feedback mechanism was identified where Aβ production is promoted by cholesterol while de novo cholesterol biosynthesis is hindered by high cellular $A\beta_{1-40}$ concentrations [31]. Cholesterol-lowering drugs such as 3-hydroxy-3-methylglutaryl-CoA reductase inhibitors may reduce the risk of AD [32], although controversial results have been reported in parallel [33].

Remarkably, brain capillary endothelial cells (BCEC) express APP and the whole APP processing machinery such as C-terminal fragments (CTFs, derived from α-secretase- and β-secretase-mediated processing of APP), neuroprotective sAPPα, and Aβ oligomers [34,35]. Furthermore, BCEC express (i) receptors or transporters involved in HDL metabolism such as SR-BI, ABCA1, ABCG1, (ii) PLTP (involved in HDL remodelling [36]) and (iii) synthesize HDL-associated apolipoproteins like apoA-I in porcine BCEC (pBCEC) [37], apoE in murine BCEC (mBCEC), apoM [38], and apoJ [35]. Nuclear receptor agonists for liver X receptors (LXRs) and peroxisome-proliferator activated receptors (PPARs) promote cholesterol efflux as well as HDL formation and remodelling at the BBB [37,39]. Both, LXR agonists as well as simvastatin (an inhibitor of endogenous cholesterol biosynthesis) modulate APP processing and Aβ production [34,35].

As PPARs form obligate heterodimers with retinoid X receptor (RXR), and particularly PPARα represents a promising target in neurodegenerative diseases [40], we here applied the PPARα agonist [41], astaxanthin (Asx), in order to compare risks, benefits, and the potential of such treatment to bexarotene (Bex). Asx (Supplementary Table S1), a natural carotenoid, exerts anti-oxidative, anti-inflammatory, and neuroprotective effects [42]. Thus, Asx can easily cross the BBB and has been reported to significantly ameliorate BBB integrity [43]. Recent studies with Asx report on multiple neuroprotective effects [44] against oxidative stress [45] as well as anti-inflammatory [43] and anti-apoptotic properties [46]. Furthermore, Asx also significantly reduced impairment of spatial memory in Swiss albino male mice [47].

Bex (Supplementary Table S1) [48] is a RXR agonist, approved by the US FDA to treat advanced cutaneous T cell lymphomas [49], some other types of cancer, and psoriasis [50,51]. Implications for RXR-directed therapeutic strategies are widely discussed in AD [52]. In a ground-breaking study, Cramer and coworkers [53] reported that oral administration of Bex to mutant, APP-overexpressing mice, APPswe/PS1ΔE9 (APP/PS1), rapidly cleared > 50% of cerebral Aβ plaques within just 72 h and reversed behavioural and cognitive deficits in these mice. In parallel, Bex treatment promoted expression of ABCA1 in hippocampus and cortex of APP/PS1 mice and reversed apoE4-induced neuronal impairment [53]. Interestingly, increased Aβ clearance was also observed by OAB-14, a Bex derivative, in APP/PS1 mice [54] and with Nitrostyrene derivative Z-10 (a first identified nitro-ligand of RXRα) and its 2-ethyoxyl substituted derivative Z-36 [55]. However, other studies failed to confirm a Bex-mediated rapid clearance of Aβ from the brain [56–58]; thus the underlying mechanisms of Aβ clearance are not completely understood.

The aim of the present study was to investigate effects of Asx and Bex, and underlying biochemical mechanisms, on pathways of APP processing, Aβ transport across the BBB, and cholesterol homeostasis in a well-established in vitro model of the BBB consisting of pBCEC [59]. Complementary in vivo studies were performed to clarify if the nuclear receptor agonists, Asx and Bex, when fed to 3xTg AD mice (that overexpress *APPswe*, and Tau*P301L* transgenes on a PS1*M146V* knock-in background) will exert similar effects on cholesterol and Aβ transport pathways and on Aβ load in cerebrovascular endothelial cells.

2. Materials and methods

2.1. Materials

Cell culture flasks, plates, and other plastic ware were from Greiner Bio-One. Cell culture medium M199 and MCDB131, minimal essential medium (MEM), Dulbecco's modified Eagle's medium (DMEM)/Ham's F-12, porcine serum, and dispase were from Life technologies; collagen G (from bovine calf skin) was from Biochrome, and cell culture additives were from PAA laboratories. Collagenase/dispase was from Roche Applied Science. Transwell multiwell plates (polyester membrane inserts, 0.4 μm pore size), as well as hydrocortisone and Percoll (pH 8.5–9.5), were from Sigma-Aldrich. Bex was from Calbiochem (Merck Millipore) and LC Laboratories and Asx was from AdipoGen or Sigma-Aldrich. Corn oil was from Sigma-Aldrich. Dextran was from VWR. [^{14}C]-sucrose, Ultima Gold scintillation cocktail, and scintillation vials were from Perkin Elmer. [^{125}I]-($A\beta_{1-40}$) was from Phoenix Pharmaceuticals. PA 452 (an RXR antagonist) was from Tocris. Probucol (P9672, an anti-hyperlipidemic drug) and GW 6471 (a PPARα antagonist) were from Sigma-Aldrich. DharmaFECT 1 Transfection Reagent and ON-TARGETplus Non-targeting Control siRNAs were from Dharmacon.

Targeting siRNAs for porcine LRP-1 (5′-GGAGGAUGACUGUGAA CAU-3′, 5′-ACAACGCUGUCGCCUUGGA-3′ and 5′-CCUGUACUGGUGU GACAAA-3′), were from Microsynth. Diethylamine (DEA) and formic acid (FA) were from Sigma-Aldrich.

Polyvinylidene fluoride (PVDF; 0.45 μm) transfer membranes were from GE healthcare. Antibodies were from Sigma-Aldrich (β-actin Cat#A2066, goat anti-mouse-HRP Cat#A0168, anti-amyloid precursor protein, C-terminal A8717), Millipore (A11 rabbit anti-Amyloid Oligomer, αβ, oligomeric, Cat# AB9234), BioLegend (purified anti-β-Amyloid, 1–16 antibody, Clone: 6E10, Cat# 803002), Abcam (anti-ABCA1 antibody [AB·H10] ab18180) and (anti-ABCG1 [EP1366Y] antibody ab52617) and (anti-LRP-1 antibody ab192308). Polyclonal rabbit-anti-human apoA-I antiserum was from Behring. Goat anti-rabbit cyanine-3 (Cy-3) antibody was from Jackson ImmunoResearch Lab. Polyclonal rabbit anti-human von Willebrand Factor (vWF) and Cytomation antibody diluent with background reducing components were from Dako Inc. Both non-immune mouse and rabbit IgGs were from Millipore Corp. Donkey anti-rabbit Dylight 488 (green) were from BioLegend Inc. Vectashield mounting medium was from Vector Lab, Inc.

PCR reagents were from Bio-Rad and primers were from Invitrogen. Pre-validated primers were from Qiagen (QuantiTect Primer Assay). All other reagents and chemicals were either from Sigma-Aldrich or Merck.

2.2. Isolation and culture of pBCEC

pBCEC, used as an in vitro BBB model, were isolated according to the protocol [60] with minor adaptations [36] from 3 hemispheres of freshly slaughtered pigs (6 months old). After removal of the meninges and secretory areas of the porcine brain, pBCEC were isolated from the remaining cerebral cortex by sequential enzymatic digestion and centrifugation steps. In brief, the cortex was minced and dispase (70 mg/brain) in 40 ml M199 medium (containing 1% penicillin/streptomycin [P/S], 1% gentamycin, 1 mM L-glutamine) was added and incubated at 37 °C in the water bath for 1 h with gentle stirring. Dextran solution (150 ml) was added and the suspension was centrifuged (6800 × *g*, 10 min, 4 °C). The pellet was resuspended in M199 medium (containing 1% P/S, 1% gentamycin, 1 mM L-glutamine and 10% porcine serum) and the capillaries were disrupted mechanically by filtering the suspension through a nylon mesh and enzymatically by adding 350 μl collagenase/dispase. The suspension was carefully pipetted onto a Percoll bi-phase gradient (15 ml of 1.07 g/ml and 20 ml of 1.03 g/ml Percoll solution) and centrifuged (1300 × *g*, 10 min) in a swinging bucket rotor. Endothelial cells were isolated from the interphase by aspiration and cells were plated onto collagen coated 75 cm^2 cell culture flasks in M199 medium (containing 1% P/S, 1% gentamycin, 1 mM L-glutamine, and 10% porcine serum). After 24 h, endothelial cells were washed twice with PBS and cultured in M199 containing 10% porcine serum, 1% gentamycin, 1% P/S, and 1 mM L-glutamine. After 3 days in culture, the cells were split (using trypsin, 0.5%) onto collagen-coated multiwell plates or transwell filters. All cell culture incubations were performed at 37 °C in humidified air containing 5% CO_2. To establish polarized pBCEC, cells were plated onto collagen-coated (120 μg/ml) Transwell® (6- or 12-well) cell culture dishes at a density of 40,000 [39]. The tightness of the transwell culture was assessed by measuring trans-endothelial electrical resistance (TEER) using an EndOhm tissue resistance measurement chamber and an EndOhm ohmmeter (World Precision Instruments). TEERs of collagen-coated, cell-free filters were used for blank measurements. After 2 to 3 days in culture, when TEERs reached ≥70 Ω/cm^2, the formation of tight junctions was induced by switching to DMEM/Ham's F-12 medium, containing 550 nM hydrocortisone, 1% P/S and 0.7 mM glutamine. After 16 to 20 h of induction, filters with ~300–1000 Ω/cm^2 were used for experiments.

2.3. Animal studies

Animal experiments were performed after ethical approval of the Austrian Department of Science, Research and Economy (approval number 66010/0052-WF/V/3b/2015). Triple transgenic AD (3xTg AD) mice, harbouring the mutant genes APP $_{Swe}$/MAPT $_{P301L}$/PSEN1 $_{M146V}$ were originally obtained from the Jackson Laboratory. Progressively generated plaques and tangles are present in the brains of these mice [61]. Since female 3xTg AD mice were reported to establish significantly larger Aβ burden and behavioural deficits compared to age-matched males [62,63], we used females in the present study. Female 3xTg AD and non-transgenic C57/BL6 (wild-type, non-Tg) mice were maintained at a 12 h light/12 h dark cycle in a humidity- and temperature-controlled environment with free access to chow diet (Ssniff, Germany). Prior to treatment, blood was collected from the submandibular vein. Two individual studies were performed:

In *study I*, < 1-year-old (32–49 weeks old) female 3xTg AD mice were gavaged for 6 days with vehicle (10% DMSO in corn oil [v/v]; vehicle control group, n = 10), Bex (100 mg/kg in DMSO/corn oil; n = 9), or Asx (80 mg/kg in DMSO/corn oil; n = 8) and compared to non-Tg mice (37–49 weeks; n = 5 for vehicle control group; n = 6 for Bex; n = 7 for Asx).

In *study II*, aged (68–92 weeks old) female 3xTg AD mice were gavaged for 6 days with vehicle (n = 8), Bex (100 mg/kg; n = 6), or Asx (80 mg/kg; n = 8). Body weights were assessed before treatment, at day 4, and before sacrification.

On day 7, mice were fasted for 6 h prior to sacrification using a gentle CO_2 stream. EDTA blood samples were taken via cardiac puncture and plasma lipids were measured enzymatically using colorimetric assay kits (DiaSys Diagnostic Systems). Murine brains were removed from the skull and divided into two hemispheres. One hemisphere was sliced into 3 pieces, two were frozen for protein and RNA isolation at −20 °C, the third one was snap frozen and stored at −70 °C for immunofluorescence microscopy. The other hemisphere was pooled with up to three hemispheres from mice of the same group, and mBCEC were isolated (see below) on the day of scarification.

2.4. Isolation of mBCEC

One hemisphere of each animal was used to isolate mBCEC [35] and cells from 3 hemispheres were pooled. In brief, the hemispheres were washed in phosphate-buffered saline (PBS, pH 7.4, containing 2% P/S) and the olfactory bulb was removed. Scalpel and douncer were used to mince the grey and white matter of the cortex. To isolate capillaries, the homogenate was mixed with dispase (10 mg/two hemispheres) in 5 ml MCDB131 medium (containing 2% fetal bovine serum, 1% L-glutamine

and 1% P/S), and incubated at 37 °C in the water bath for 1 h. After adding dextran (5 ml), the suspension was centrifuged (10,000 ×*g*, 10 min, 4 °C) and the pellet was resuspended in 5 ml medium and filtered through a nylon mesh (180 μM). In order to disrupt capillaries and removing the basement membrane and adhering pericytes [64], 40 μl collagenase/dispase (1 min in a water bath) was supplemented, the suspension filled up to 5 ml medium and centrifuged (900 rpm, 5 min, 25 °C). Endothelial cells were harvested using a Percoll bi-phase gradient as referred above for pBCEC. Cells were washed with PBS and stored at −20 °C for protein and RNA isolation. The purity of isolated mBCEC was confirmed by performing quantitative real-time PCR (qPCR) for mRNA expression of cell-specific markers such as cluster of differentiation 31 (CD31) for endothelial cells, aminopeptidase N (CD13) and beta-type platelet-derived growth factor receptor (PDGFRβ) for pericytes, glial fibrillary acidic protein (GFAP) for astrocytes, synaptophysin (SYP) for neurons, ionized calcium binding adaptor molecule 1 (IBA1) for microglia, and smooth muscle actin (SMA) for smooth muscle cells (Supplementary Fig. III). The lack of CD13 or PDGFRβ mRNA is indicative for the absence of pericytes in the isolated mBCEC fraction, which was highly enriched in CD31 identifying endothelial cells.

2.5. BACE activity assay

The activity of BACE1 was estimated using the fluorometric Beta-Secretase Activity Assay Kit (Abcam). A secretase-specific peptide is conjugated to two reporter molecules (EDANS, DABCYL), which are separated upon cleavage of the peptide by secretase allowing for the release of a fluorescent signal. In brief, pBCEC were incubated with either vehicle control (0.5% ethanol), Bex [100 nM] or Asx [10 nM] in serum-free medium for 24 h at 37 °C. Cells were harvested by scraping and centrifuged for 5 min at 700 ×*g*. Supernatants were discarded and 0.1 ml of ice-cold extraction buffer was added, followed by treatment with lysis buffer, and subsequent determination of the activity using a fluorimeter (Flexstation 2 Molecular Devices) (Ex = 345 nm/Em = 500 nm) [35].

2.6. Isolation of RNA and qPCR

Primary pBCEC were grown in 6-well plates and incubated in serum-free medium (500 ml Earle's medium M199 1×, 1% P/S, 1 mM L-glutamine) in the absence or presence of vehicle control (0.5% ethanol), Bex [10 and 100 nM], or Asx [1 and 10 nM] for 24 h at 37 °C. For RNA isolation [35], pBCEC from each well were lysed in 1 ml TriReagent RT (Molecular Research Centre). Whole mouse brain tissue (~50 mg) was minced after adding 1 ml TriReagent RT for 3 × 10 s using an Ultra Turrax tissue homogenizer. RNA concentration was quantitated using a Nanodrop (Thermo Scientific). cDNA was synthesized using the High Capacity Reverse Transcriptase kit (Life Technology). qPCR was performed on a CFX96 PCR detection system (Bio-Rad) using iQ SYBR Green supermix (Bio-Rad). The qPCR program comprised one cycle at 95 °C for 3 min, 40 cycles of 95 °C for 10 s, 60 °C for 20 s, 72 °C for 40 s. Primers used are listed in Table 1. Hypoxanthine phosphoribosyltransferase 1 (HPRT1) was used as a housekeeping gene. Gene expression levels were normalized to HPRT1 using the 2-ΔΔCT method [65].

2.7. SDS-PAGE and immunoblotting

Primary pBCEC were grown in 6-well plates and incubated with serum-free medium (500 ml Earle's medium M199 1×, 1% P/S, 1 mM L-glutamine) containing control (0.5% ethanol), Bex [10,100 nM] or Asx [1,10 nM] for 24 h at 37 °C. Cellular lysates and trichloroacetic acid (TCA) precipitates of secreted proteins were prepared after 24 h of incubation [38]. Immunoblot analysis of mBCEC was performed using total cell protein lysates of isolated cells. Protein concentrations were measured by using the bicinchoninic acid (BCA) assay (Thermo Scientific), lysates mixed with sample buffer, and proteins denatured at 95 °C for 5 min in a thermocycler. Equal amounts of protein (20 μg) was loaded onto gradient NuPage® Novex 4–12% Bis-Tris Midi Gels (Thermo Scientific) and subjected to SDS-PAGE under reducing conditions as described [66]. For immunoblotting, proteins were electrophoretically transferred [67] to 0.45 μm PVDF membranes (GE healthcare). After blocking with 10% non-fat dry milk (Bio-Rad) in Tris-buffered saline containing Tween 20 (TBST) for 1 h, the membranes were probed with the following primary antibodies diluted in TBST containing 5% milk powder: anti-β-actin (1:2000), rabbit anti-Amyloid Oligomer antibody (A11) (1:5000), anti-β-Amyloid 6E10 (1:1000), anti-ABCA1 (1:2000), anti-ABCG1 (1:1000), rabbit-anti-apoA-I antiserum (1:1000) [68], anti-LRP-1 (1:10000), anti-amyloid precursor protein, anti-C-terminal A8717 (1:1000). After washing, membranes were incubated with goat anti-rabbit IgG-HRP (Bio-Rad) (1:5000) or goat-anti-mouse IgG-HRP (Sigma Aldrich) (1:5000) as secondary antibodies.

In parallel, Aβ was extracted from murine brains and immunoblotting was performed for both insoluble (FA) and soluble (DEA) Aβ fraction. Both fractions were loaded to 12% NuPage (Thermo Fisher) gels and electrophoresis was performed using MES buffer (ThermoFisher). Blotting was carried out using Tris-glycine buffer (25 mM Tris, 0,5 M glycine, 20% methanol) and nitrocellulose membrane (GE Healthcare Protran BA83) for 3 h, 50 mA at 4 °C. After blotting, membranes were stained with Ponceau S. Then, membranes were boiled for 5 min in PBS in a microwave in order to unfold respective epitopes and blocked (5% milk powder, 1× TBS) for 1 h. Blots were probed using 6E10 as primary antibody (1:750) and goat-anti-mouse IgG-HRP as secondary antibody. Chemiluminescent signals were

Table 1
Primer sequences, forward (F) and reverse (R) for porcine (ss) and murine (mm) genes used for qPCR analysis.

Gene	Sequence (5′-3′)	Amplicon size (bp)
ss*ADAM10*	F, AGCAACATCTGGGGACAAAC R, CTTCCCTCTGGTTGATTTGC	219
ss*BACE1*	F, TGGACTGCCTCATGGTGTG R, GTGACCAAAGTGAACCACCG	155
ss*HPRT1*	F, AGGACCTCTCGAAGTGTTGG R, CAGATGGCCACAGGACTAGA	247
ss*LRP-1*	F, GCAGATGTATCAACATCAACTGG R, GGGTGCTAGAGCAAGAGTGG	98
ss*ABCA1*	F, GCCATTCTCCGGGCCAAC R, GGCTTCACGCCGCTGAT	252
ss*APOA-I*	F, GATGCGATCAAAGACAGTGG R, CTGTCCCAGTTGTCCAGGAG	98
mm*LRP-1*	F, CCGCATCTTCTTCAGTGACA R, ACAGAGCCCACATTTTCCAC	96
mm *ABCA1*	F, ATTGCCAGACGGAGCCG R, TGCCAAAGGGTGGCACA	103
mm *APOE*	F, CTGACAGGATGCCTAGCCG R, CGCAGGTAATCCCAGAAGC	107
mm CD31	F, AGGCTTGCATAGAGCTCCAG R, TTCTTGGTTTCCAGCTATGG	278
mm CD13	F, CCCCGGGGCTGCTGTTCTTT R, ACCACCCGCTCCTTGTTGCTAATG	1208
mm GFAP	F, TCCTGGAACAGCAAAACAAG R, CAGCCTCAGGTTGGTTTCAT	224
mm SYP	F, CATTCAGGCTGCACCAAGTG R, TGGTAGTGCCCCCTTTAACG	60
mm IBA1	F, GGATTTGCAGGGAGGAAAAG R, TGGGATCATCGAGGAATTG	92
mm SMA	F, CTGACAGAGGCACCACTGAA R, GAAATAGCCAAGCTCAG	285
mm PDGFRβ	F, AGCTACATGGCCCCTTATGA R, GGATCCCAAAAGACCAGACA	367
mm HPRT1	F, GCCTAAGATGAGCGCAAGTTG R, TACTAGGCAGATGGCCACAGG	101
mm*HPRT1* mm*BACE1*	QUANTITECT PRIMER ASSAY (QIAGEN)	

developed using ECL (Bio-Rad) and detected and imaged using a ChemiDoc system (Bio-Rad). Immunoreactive bands were quantitated using ImageLab software (version 5.2.1, Bio-Rad).

2.8. Purification of plasma HDL and apoA-I

HDL subclass 3 (HDL_3, 1.125–1.21 g/ml) was isolated from fresh EDTA-plasma obtained from healthy, female volunteers by KBr-density gradient ultracentrifugation [69]. HDL_3 was stored at 4 °C and desalted before use with PBS (pH 7.4) using PD10 size-exclusion column chromatography. Protein content was determined by Qubit, Quant-iT Protein Assay Kit. ApoA-I was isolated from delipidated total HDL by size-exclusion chromatography on a Sephacryl S-200 column 3 × 150 cm (GE healthcare) as described [70].

2.9. Radiometric assay for cholesterol efflux

Primary pBCEC were cultured in 12-well plates. After reaching 70–80% confluency, the cells were labeled with 0.5 μCi/ml [^{3}H]-cholesterol in M199 medium and incubated at 37 °C for 24 h [36]. Where indicated (figure legends), cells were then pre-incubated with RXR antagonist PA 542 [10 μM] and PPARα antagonist GW 6471 [10 μM] for 15 min, and incubated in the presence of vehicle control (0.5% ethanol), Bex [100 nM], Bex with PA 542 or Asx [10 nM], Asx with GW 6471 in serum-free medium (500 ml Earle's medium M199 1 ×, 1% P/S, 1 mM L-glutamine) for 16 h at 37 °C. Then cells were rinsed with PBS, and cholesterol acceptors such as HDL_3 (200 μg/ml) or apoA-I (10 μg/ml) were added in fresh serum-free medium. Aliquots of cell supernatants (200 μl) were taken at the indicated time points and analysed by β-counting. Cells were washed twice with ice-cold PBS and lysed in 0.3 M NaOH over night at 4 °C. Remaining [^{3}H]-cholesterol radioactivity in the cell lysates was counted, and total cellular protein concentration was quantified using the Qubit fluorometer (Quanti-IT protein assay kit, Invitrogen). Cholesterol efflux was expressed as cpm/mg cell protein in the supernatants relative to the total counts in the supernatants plus cell lysates.

2.10. Quantitation of cellular cholesterol levels

pBCEC grown in 6-well plates were incubated in serum-free medium containing vehicle control (0.5% ethanol), Bex [100 nM] or Asx [10 nM] for 24 h. Cells were rinsed twice with PBS and incubated for 30 min under gentle agitation with cholesterol reagent (Greiner Bio-one) in the presence of 5 mg/ml enhancer sodium 3,5-dichloro-2-hydroxybenzenesulfonate (DHB; Sigma Aldrich). Absorbance (at 562 nm) was measured on a photometer with Magellan software (Tecan), and values obtained were normalized to intracellular protein content [34].

2.11. Radiometric assay for cholesterol biosynthesis and esterification

Primary pBCEC were incubated with [^{14}C]-acetate (2 μCi/ml) in the presence of vehicle control (0.5% ethanol), Bex [100 nM] or Asx [10 nM] in serum-free medium for 24 h. Incorporation of [^{14}C]-acetate into cellular cholesterol and cholesterol esters was determined as previously described [34]. Briefly, cells were rinsed twice in PBS and cellular lipids were extracted by incubation in n-hexane/isopropanol (3:2, v/v) (2 × 1 ml for 30 min, gently agitating at 25 °C). Lipid extracts were dried under a stream of nitrogen and resuspended in 50 μl of chloroform/methanol (2:1, v/v). Aliquots of the samples were counted on a β-counter to obtain total counts/well. Lipid extracts were loaded onto silica TLC plastic plates (Merck). For separation of free and esterified cholesterol, n-hexane/diethylether/acetic acid (70:29:1, v/v/v) was used as the mobile phase. Standards (Sigma Aldrich) for all lipid classes (1 mg/ml) were subjected in parallel to TLC plates. Respective lipid spots were stained with iodine vapour, cut out, and radioactivity was determined by β-counting (Liquid Scintillation Analyzer, Packard). Total counts per sample were normalized to intracellular protein content (estimated using the Qubit fluorimeter and the Quant-iT Protein Assay kit, Invitrogen).

2.12. Aβ uptake studies

Primary pBCEC were grown in collagen-coated 24-well plates and incubated in the presence of vehicle control (0.5% ethanol), Bex [100 nM] or Asx [10 nM] for 24 h. Aβ uptake by pBCEC was measured as recently described [35]. In brief, 100 μl of $A\beta_{1–40}$ [1 mg/ml] was labeled fluorescently by incubating with 3 μl Alexa Fluor 488 5-TFP for 1 h at 37 °C in 18 μl carbonate-bicarbonate buffer. Unbound fluorescent dye was removed via size-exclusion chromatography on a PD-10 column [34]. Alexa-Aβ secondary structure was characterized by immunoblotting and confirmed to be identical to unlabelled $A\beta_{1–40}$ (not shown). After 24 h, cells were incubated with Alexa Fluor 488 labeled $A\beta_{1–40}$ [0.5 μg/ml] for 2 h at 37 °C, and fluorescence was measured in the cellular supernatants at 490–525 nm using the Promega Glomax detection system. Cells were lysed by adding 0.3 M NaOH and cellular protein content was measured using the Qubit fluorometer (Quant-IT protein assay kit) [35]. Alternatively, [^{125}I]-$A\beta_{1–40}$ uptake was also measured in parallel with Aβ transport studies (see below).

2.13. Aβ transport studies

Primary pBCEC were grown on collagen-coated [120 μg/ml] 12-well transwell filters, incubated in the presence of vehicle control (0.5% ethanol), Bex [100 nM], or Asx [10 nM] for 24 h in DMEM/Ham's F12 medium containing 1% P/S, 0.25% glutamine and 500 nM hydrocortisone (Sigma Aldrich). In parallel, the increase in TEER was measured (as described above in Section 2.2). To assess Aβ transport from across the in vitro BBB model, 0.3 nM of [^{125}I]-$A\beta_{1–40}$ and 100 nM [^{14}C]-sucrose (as paracellular transport control, which is not taken up by cells) was added to the basolateral compartment. Transport of [^{125}I]-$A\beta_{1–40}$ from the basolateral ('brain parenchymal') to the apical ('blood') compartment was measured after 2 h. From each basolateral (input) and apical (acceptor) compartment, 100 μl or 50 μl were taken to count radioactivity of [^{125}I]-$A\beta_{1–40}$ or [^{14}C]-sucrose. To measure transcytosis of intact [^{125}I]-$A\beta_{1–40}$ to the luminal side, 50 μl of apical media were subjected to 15% TCA precipitation and incubated for 10 min at 4 °C (to precipitate Iodine bound Aβ). Samples were then centrifuged at 10,000 × *g* for 10 min at 4 °C and radioactivity associated to pellets was counted on a γ-counter, the supernatant was transferred to a new vial, the same procedure was repeated with basolateral samples and uptake of [^{125}I]-$A\beta_{1–40}$ was calculated as the percentage of cpm/mg cell protein in the pellet of cell lysates relative to the cpm/mg of supernatant. In parallel, 50 μl of apical media were counted on a β-counter with 5 ml Ultima Gold scintillation cocktail to examine the passive diffusion of [^{14}C]-sucrose across the BBB. Transcytosis quotient (TQ) was calculated as followed [35]:

$$\text{Aβ TQ} = \frac{\frac{[125\text{I}]\ \text{Aβ}\ acceptor}{[125\text{I}]\ \text{Aβ}\ input}}{\frac{[14C]\ \text{sucrose}\ acceptor}{[14C]\ \text{sucrose}\ input}}$$

2.14. Cytotoxicity assay

The cytotoxicity assay was performed using cell proliferation Reagent WST1 from Roche. In brief, pBCEC were seeded onto collagen-coated [60 μg/ml] 96-well plates. Upon reaching confluence, cells were treated for 24 h with vehicle control (0.5% ethanol), Bex [100 nM] or Asx [10 nM]. The absorbance of the formazan product was measured photometrically at 450 nm and 650 nm by Magellan software (SUNRISE TECAN).

2.15. Reactive oxygen species (ROS) assay

pBCEC were cultured in collagen-coated [60 μg/ml] 12-well plates and treated with control (0.5% ethanol), Bex [100 nM] or Asx [10 nM] for 24 h. ROS measurement was carried out using H_2DCFDA fluorescent dye as described [71]. Fluorescence was measured at excitation and emission wavelengths of 485 and 530 nm, respectively, using the Promega Glomax detection system. The protein content of cell protein lysates was determined using BCA™ protein assay kit and fluorescence was normalized to protein content.

2.16. LRP-1 gene-silencing in pBCEC

Primary pBCEC were cultured in 6-well plates for 3 days to reach ~70% confluency and transfected with DharmaFECT transfection reagent 1 following manufacturer's instructions and as described with minor modifications [38]. In brief, three targeting siRNAs for each target gene (i.e. porcine *LRP-1* [5′-GGAGGAUGACUGUGAACAU-3′, 5′-ACAACGCUGUCGCCUUGGA-3′ and 5′-CCUGUACUGGUGUGAC AAA-3′]) were pooled in nuclease-free water to obtain 5 μM stock solutions. The stocks were then diluted (1:10) in serum-free (SF) medium, Dharmafect was diluted in SF medium (1:40), each was incubated for 5 min at RT, both dilutions were mixed and incubated for 25 min at RT. Medium in the 6-well plate was changed to 1.6 ml complete medium (M199, containing 10% horse serum, without antibiotics). Transfection mix (400 μl) was added dropwise to each well and incubated for 24 h in 37 °C. Cells were treated with Bex [100 nM] and Asx [10 nM] for another 24 h in 37 °C.

2.17. Immunofluorescent staining on snap frozen mouse brain sections by using 6E10 and oligomer (A11) antibodies

Staining was performed on 18 μm cryosections from mouse brain tissues. Sections were fixed in cold acetone (5 min) and air-dried (20 min) prior to immunofluorescent staining. Sections were washed with TBST (pH 7.4), blocked with Ultra-V block for 7 min and then incubated with polyclonal rabbit anti-Aβ, A11 (Ab9234, 8 μg/ml) or mouse anti-β-Amyloid (6E10, 5 μg/ml, SIG-39320) as primary antibodies for 1 h at 25 °C. Primary antibodies were diluted with Dako antibody diluent to reduce background staining. Sections were washed for 5 min with TBST and goat anti-rabbit Cy-3 (red, 1.88 μg/ml, 30 min) was used as secondary antibody. All incubation steps were performed in a dark moist chamber at 25 °C. Slides were washed by TBST. DAPI was added to the slides (20 min) for nuclear staining. Sections were rinsed again with TBST and mounted with Vectashield mounting medium. To acquire and analyse computerized images of sections and cells, a Leica DM4000 B microscope (Leica Cambridge Ltd) equipped with Leica DFC 320 video camera was used. Non-immune rabbit IgG was used as negative control.

2.18. Vascular endothelial cell double-staining of snap frozen mouse brain sections

Double staining of vWF (a specific endothelial cell marker) and Aβ was carried out on 18 μm cryosections of mouse brain samples. Tissue sections were fixed with 4% paraformaldehyde for 10 min, rinsed in distilled water prior to immunofluorescence staining. All incubations were performed at 25 °C. Sections were washed with TBST (pH 7.4), blocked with donkey serum for 1 h and incubated with primary antibody for 1 h at 25 °C. Mouse anti-β-Amyloid (6E10, 5 μg/ml) and rabbit anti-vWF (0.16 μg/ml) antibodies were used. All incubation steps were performed in a dark moist chamber at 25 °C. Slides were rinsed by TBST and donkey anti-mouse Cy-3 (red, 1.88 μg/ml) and donkey anti-rabbit Dylight 488 (green, 1.66 μg/ml) were used as secondary antibodies (30 min). Slides were washed again with TBST and DAPI was added for 20 min for nuclear staining. Sections were rinsed again with TBST and mounted with vectashield mounting medium. Both, non-immune mouse or rabbit IgG were used as negative controls. To acquire and analyse computerized images of sections and cells, a Leica DM4000 B microscope (Leica Cambridge Ltd) equipped with Leica DFC 320 video camera was used.

2.19. Aβ extraction from mice brain

Frozen brain cortical hemispheres from female 3xTg AD mice and wild-type C57BL6 mice (non-Tg) were used. Extraction of both soluble (DEA: Aβ isoforms and APP) and insoluble (FA: Aβ isoforms associated with plaques) proteins were performed exactly as described [72]. In brief, mechanically homogenized brain tissue (250 μl) were mixed with 0.4% DEA solvent (250 μl), (DEA: 1 ml of 5 M NaCl and 50 ml of ddH_2O) and were centrifuged at 135,000 × *g* for 1 h at 4 °C, the supernatant (425 μl) was neutralized with 0.5 M Tris-HCl (42.5 μl) and stored at −80 °C. The pellet was sonicated on ice (1 min) in 95% FA (~20 s with 15 mA amplitude) until the pellet dissolved, centrifuged at 109,000 × *g* for 1 h at 4 °C. The supernatant (105 μl) was neutralized with FA neutralization buffer (1 M Tris, 0.5 M Na_2HPO_4 and 0.05% NaN_3) and the samples were stored at −80 °C. Immunoblotting was performed to analyse Aβ species and to evaluate the amyloid burden in mice.

2.20. Nissl staining on snap frozen mouse brain sections

Staining was performed on 18 μm cryosections from mouse brains. Sections were fixed in 4% paraformaldehyde (15 min) and stained with 0.1% thionine (5 s). Sections were washed with ddH_2O. Slides were dehydrated and mounted with permount. To acquire and analyse computerized images of sections, a Motic microscope (MOTIC Deutschland GmbH) equipped with Moticam Pro 285B camera was used.

2.21. Statistical analysis

Experiments were performed at least three times in triplicates and data are expressed as means ± SEM unless stated otherwise. Statistical significances (*$p \leq 0.05$; **$p \leq 0.01$; ***$p \leq 0.001$; ****$p \leq 0.0001$) were determined by one-way or two-way ANOVA performed by using Prism 6 software (Graphpad version 6).

3. Results

3.1. Asx and Bex shift APP processing towards the non-amyloidogenic pathway in pBCEC

To study effects of both drugs on mRNA expression levels for APP and processing enzymes, as well as protein levels of Aβ, pBCEC were treated for 24 h with vehicle (0.5% ethanol), Bex [10,100 nM] or Asx [1,10 nM]. A dose-dependent up regulation of APP mRNA levels by 1.2 ± 0.04-fold with Bex [10 nM], 2.2 ± 0.10-fold by Bex [100 nM] (Fig. 1A) was observed. One-way ANOVA for treatment showed a significant effect ($p \leq 0.0001$). Significantly elevated APP mRNA levels by 1.2 ± 0.04-fold with Asx [1 nM] and 1.7 ± 0.04-fold with Asx [10 nM] (Fig. 1B) ($p = 0.0008$) were observed. In parallel, TCA-precipitated protein levels of sAPPα were increased by 5.9 ± 0.92 ($p = 0.0079$) with Bex [100 nM] (Fig. 1C) and by 7.7 ± 1.65 ($p = 0.0004$) with Asx [10 nM] treatments (Fig. 1D). Further, a significant increase in relative *ADAM10* mRNA levels in response to Bex (1.5 ± 0.20-fold at [10 nM], 1.8 ± 0.18-fold at [100 nM]) (Fig. 1E) ($p = 0.0435$) and Asx (1.6 ± 0.11-fold at [1 nM] and 2.2 ± 0.03-fold at [10 nM]) (Fig. 1F) ($p = 0.0001$) was observed. Interestingly, *BACE1* mRNA was down regulated upon treatment with Bex [100 nM] by 41 ± 7.6% (Fig. 1G) ($p = 0.0007$) and Asx (1 nM by 17 ± 0.6%; Asx 10 nM by 22 ± 1.5%) (Fig. 1H) ($p = 0.0092$). Accordingly, total BACE activity was significantly reduced upon treatment of pBCEC with Bex

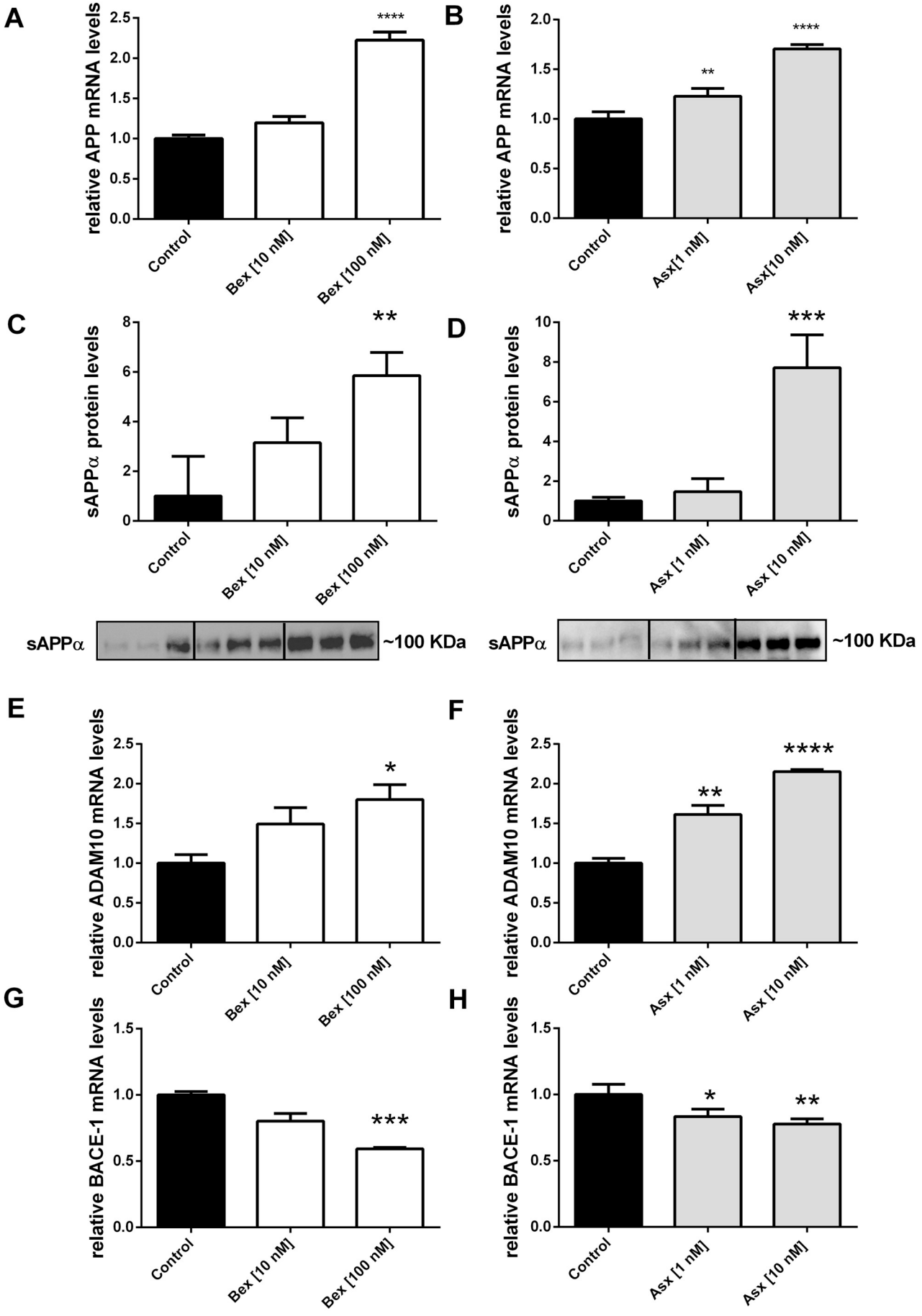

(caption on next page)

Fig. 1. Bex and Asx inhibit amyloidogenic APP processing and enhance the non-amyloidogenic pathway in pBCEC. (A–B, E–H) pBCEC cultured on 6-well plates were incubated with 0.5% ethanol (vehicle control), Bex [10 and 100 nM] or Asx [1 and 10 nM]. Total RNA was isolated, reverse-transcribed, and subjected to qPCR analysis using SYBR Green technology and HPRT1 as house-keeping gene. The ΔΔCt method was applied to quantify relative mRNA expression levels of *APP*, *ADAM10* and *BACE-1*. Data shown are mean ± SEM of 3 independent experiments performed in triplicates (*p ≤ 0.05; **p ≤ 0.01; ***p ≤ 0.001; ****p ≤ 0.0001 vs controls). (C–D) Proteins were extracted from cells and TCA-precipitated from supernatants, separated by SDS-PAGE, and levels of secreted sAPPα (normalized to Ponceau stained bands) were detected by immunoblot experiments using 6E10 as primary antibody. One representative blot out of 3 is shown. The graphs represent densitometric analysis, data shown are mean ± SEM of 3 experiments performed in triplicates (**p ≤ 0.01; ***p ≤ 0.001 vs controls). (I) pBCEC cultured in 25 cm^2 flasks were incubated with 0.5% ethanol (control), Bex [100 nM] or Asx [10 nM] for 24 h. BACE-1 activity was measured by using the fluorometric BACE-1 activity assay kit (Abcam) using 100 μg of total protein content. Data represent mean ± SEM from 3 experiments with different cell preparations performed in duplicates (*p ≤ 0.05 vs controls). (J–K) Bex and Asx reduce Aβ oligomer levels in pBCEC. Proteins were extracted from cells, separated by SDS-PAGE, and levels of Aβ oligomers (normalized to β-actin levels) were detected by immunoblot experiments using A11 as primary antibody. β-Actin was used as loading control. One representative blot out of 3 is shown. The graphs represent densitometric evaluation, data shown are mean ± SEM of 3 experiments performed in triplicates (*p ≤ 0.05 vs controls). (L–M) Bex and Asx reduce ~80 kDa 6E10-reactive APP/Aβ species in pBCEC. Proteins were extracted from cells, separated by SDS-PAGE, and level of Aβ species (normalized to β-actin levels) were detected by immunoblot experiments using 6E10 as primary antibody. β-Actin was used as loading control. Data shown are mean ± SD of one representative experiment out of two performed in triplicates (**p ≤ 0.01; ****p ≤ 0.0001 vs controls).

[100 nM] by 17 ± 0.6% or Asx [10 nM] by 17 ± 0.8% (Fig. 1I) (p = 0.0156). As expected in pBCEC, immunoblots for Aβ oligomers (using A11 antibody) revealed a prominent band at ~38 KDa [35], which was markedly reduced by Bex [100 nM, 36 ± 3.7%] (Fig. 1J) (p = 0.0343) and Asx [10 nM, 69 ± 4.7%] (Fig. 1K) (p = 0.0166). Strikingly, a prominent 6E10-reactive APP/Aβ species ~80 KDa band detected in vehicle-treated pBCEC lysates (and APP/Aβ species not cross reacting with C-terminal APP antibody, data not shown) was reduced by Bex [100 nM] by 90 ± 0.01% (Fig. 1L) (p < 0.0001) and almost completely disappeared upon treatment with Asx [10 nM] (Fig. 1M). These in vitro results demonstrate that both drugs significantly inhibit Aβ production in pBCEC while promoting non-amyloidogenic APP processing in parallel.

3.2. Effects of Asx and Bex on ROS levels and proliferation of pBCEC

Treatment of pBCEC with Bex [100 nM] for 24 h decreased H_2DCFDA-reactive ROS levels by 22 ± 2.6%. Asx [10 nM] significantly reduced cellular ROS levels by 61 ± 34.8% (Supplementary Fig. IIA) (p = 0.0045). This may contribute to maintain and almost improve cell viability in pBCEC undergoing treatments, as was observed with Asx and Bex when compared to control conditions (Supplementary Fig. IIB).

3.3. Asx and Bex up-regulate genes/proteins responsible for cholesterol efflux in pBCEC

We next investigated mRNA expression of ABCA1 and ABCG1 (two key transporters involved in cholesterol efflux from pBCEC) and apoA-I (an acceptor of ABCA1-mediated released cholesterol) [37,38]. Treatment with Bex [10 and 100 nM] dose-dependently increased *APOA-I* mRNA levels by 1.3 ± 0.09 and by 2.0 ± 0.07-fold (Fig. 2A) (p = 0.0002). Bex also upregulated *ABCA1* mRNA levels by 2.3 ± 0.15-fold at [10 nM] and 3.8 ± 0.36-fold at [100 nM] (Fig. 2B) (p = 0.0005). Similarly, Asx [10 nM] upregulated *ABCA1* mRNA levels by 2.7 ± 0.20-fold (Fig. 2C) (p = 0.0010). Immunoblot of TCA-precipitated proteins from the supernatants revealed that levels of secreted apoA-I were increased upon Bex treatment [100 nM] by 2.7 ± 0.24-fold (Fig. 2D) (p = 0.0034); however, Asx had neither an effect on *APOA-I* mRNA expression nor on protein levels (Supplementary Fig. IA, ID). A pronounced increase in ABCA1 protein expression levels in response to Bex [10 nM] by 4.8 ± 0.60-fold and [100 nM] by 4.8 ± 0.40-fold, respectively, was observed (Fig. 2E) (p = 0.002). Similarly, Asx increased ABCA1 protein expression levels: at low Asx concentrations [1 nM] by 2.5 ± 0.78-fold while at higher Asx concentrations [10 nM] by 3.9 ± 0.38-fold (Fig. 2F) (p = 0.0277). Furthermore, treatment of pBCEC with Asx [10 nM] slightly up regulated *ABCG1* mRNA expression by 1.2 ± 0.03 fold (Supplementary Fig. IB) (p = 0.0034), while treatment with Bex [100 nM] elevated *ABCG1* mRNA expression by 2.9 ± 0.99 fold (Supplementary Fig. IC) (p = 0.0219). Unexpectedly, treatment of cells with either Asx or Bex had no significant effect on ABCG1 protein expression (Supplementary Fig. IE, IF).

3.4. Asx and Bex enhance cholesterol release involving PPARα- and RXR-mediated activation and reduce cholesterol synthesis in pBCEC

We next investigated effects of Asx and Bex on cellular cholesterol release to apoA-I and HDL_3 and addressed a contribution of nuclear receptor-dependent mechanisms by using PPARα- and RXR-antagonists. We studied cholesterol efflux capacity of pBCEC prelabelled with [^{3}H]-cholesterol for 24 h and pre-incubated with either antagonist for 15 min before treatment with vehicle (0.5% ethanol), Bex [100 nM], Bex [100 nM] and RXR antagonist PA 542 [10 μM], Asx [10 nM], Asx [10 nM] and PPARα antagonist GW 6471 [10 μM]. ApoA-I [10 μg/ml] or apoE-free HDL_3 [200 μg/ml] were added as cholesterol acceptors to the serum-free culture media. Accordingly, results obtained here are in line with the upregulation of ABCA1 (and ABCG1 mRNA) expression: Bex [100 nM] promoted cholesterol efflux to apoA-I by 3.5-fold and 7.1-fold at 90 and 240 min, respectively. Two-way ANOVA revealed a significant effect of treatment (p ≤ 0,0001) when compared to controls. Treatment with Bex and PA 542 partially reversed this effect. Cholesterol efflux in the presence of the RXR antagonist versus untreated controls was still augmented, albeit to lower extent by (2.5-fold and 3.45-fold at 90 and 240 min; p = 0.0009) (Fig. 3A).

Asx [10 nM] increased cholesterol efflux to apoA-I by 1.3-fold and 1.6-fold at 90 and 240 min when compared to untreated controls (p = 0.0004). Treatment with Asx and GW 6471 was not significantly different from untreated controls (p = 0.4888) (Fig. 3B).

Bex [100 nM] also enhanced cholesterol efflux to HDL_3 particles by 2-fold and 1.7-fold at 90 and 240 min when compared to untreated controls (p = 0.007), whereas treatment of Bex and PA 542 was not significantly increased when compared to untreated controls (p = 0.2789) (Fig. 3C). Similarly, Asx [10 nM] increased cholesterol efflux to HDL_3 significantly by 1.9-fold and 1.5-fold at 90 and 240 min, respectively, when compared to untreated controls (p = 0,0364), whereas treatment with Asx and GW 6471 was not significantly different from untreated controls (p = 0.2866) (Fig. 3D).

To further investigate the effects of both drugs on cellular cholesterol biosynthesis and esterification, pBCEC were labeled with the cholesterol precursor molecule, [^{14}C]-acetate. TLC separation of extracted cellular lipids and subsequent measurement of radioactivity incorporated into the cholesterol and cholesterol ester fraction revealed that treatment with Bex [100 nM] significantly reduced endogenous cholesterol biosynthesis by 15 ± 1.1%; Asx [10 nM] reduced levels of free (unesterified) endogenous cholesterol by 41 ± 1.8% (Fig. 3E) (p = 0.0037). Bex [100 nM] and Asx [10 nM] reduced cholesterol ester synthesis by 51 ± 1.1% and by 36 ± 2.1%, respectively, when compared to controls (Fig. 3F) (p ≤ 0.0001). The mean ratio of cholesterol ester to total cholesterol was 1.8 ± 0.21%. In parallel, the pool (measured enzymatically with the photometric CHOD-PAP test) was

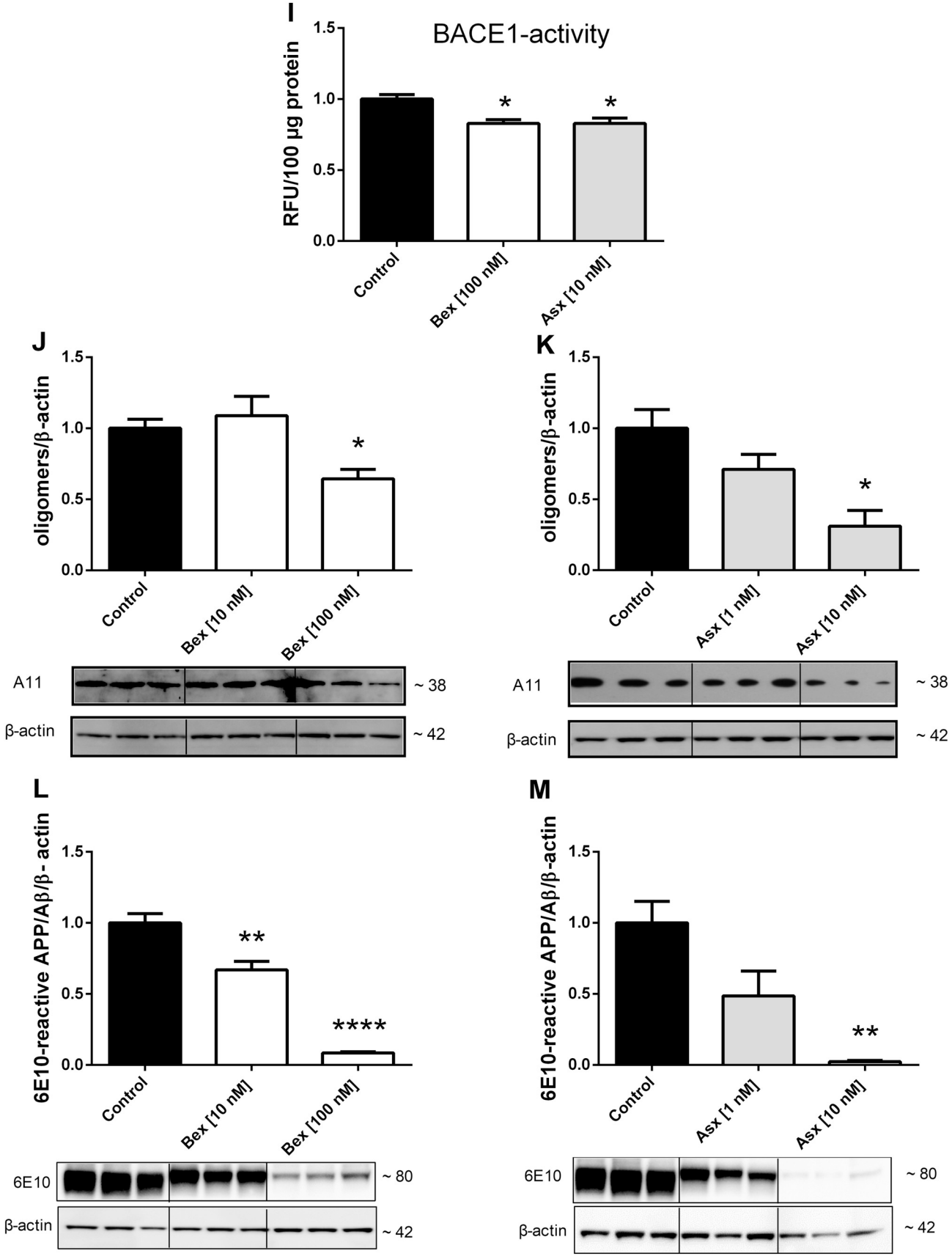

Fig. 1. (*continued*)

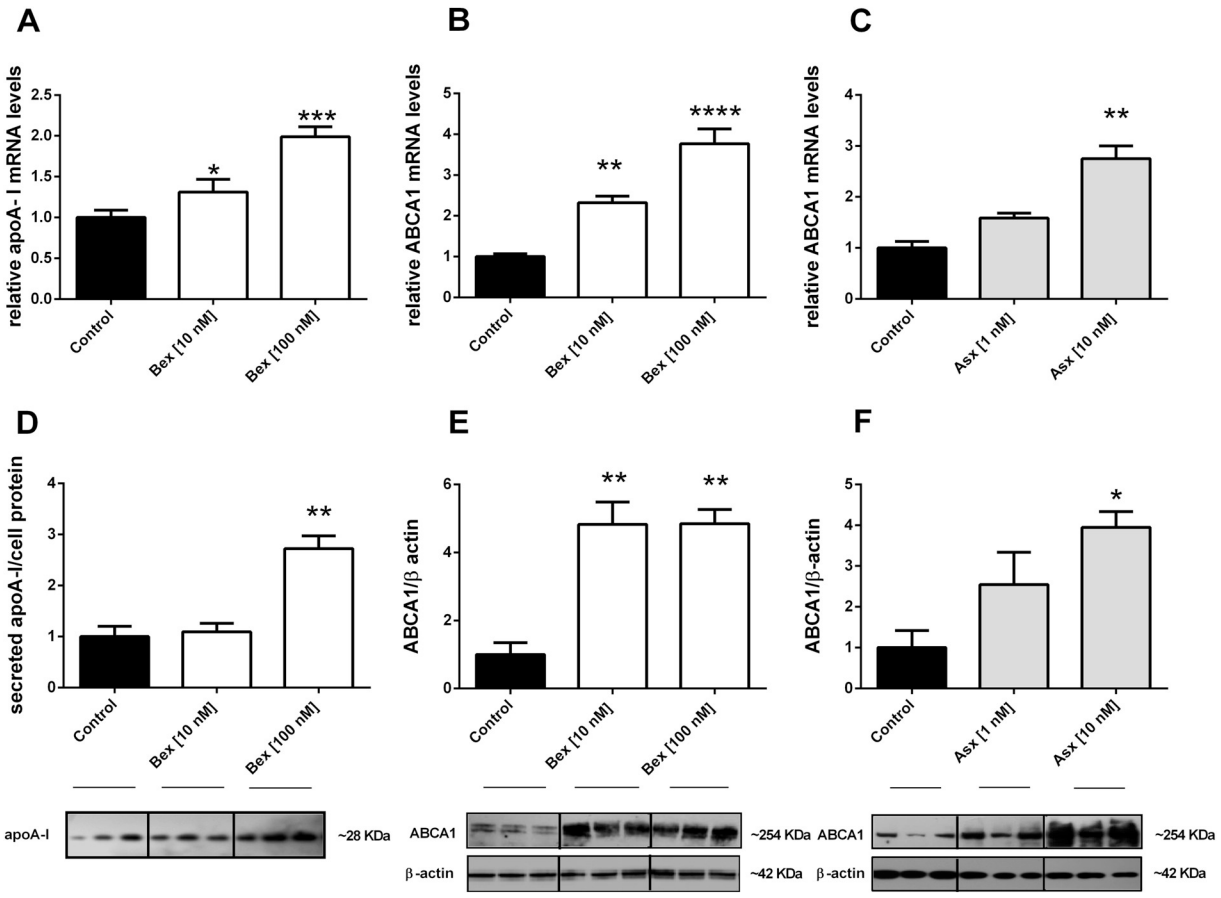

Fig. 2. Effects of Bex and Asx on ABCA1 and apoA-I expression. (A–C) pBCEC cultured on 6-well plates were incubated with 0.5% ethanol (vehicle control), Bex [10 and 100 nM] or Asx [1 and 10 nM] for 24 h. Total RNA was isolated, reverse-transcribed, and subjected to qPCR analysis using SYBR Green technology and HPRT1 as house-keeping gene. The ΔΔCt method was applied to quantify relative mRNA expression levels. Data shown are mean ± SEM of 3 independent experiments performed in triplicates (*p ≤ 0.05; **p ≤ 0.01; ***p ≤ 0.001; ****p ≤ 0.0001 vs controls). (D–F) Proteins were extracted from cells and TCA-precipitated from supernatants, separated by SDS-PAGE, and levels of secreted apoA-I (normalized to total protein content) and ABCA1 (normalized to β-actin levels) were detected by immunoblot experiments using anti-apoA-I and anti-ABCA1 as primary antibodies. β-Actin was used as loading control. One representative blot out of 3 is shown. The graphs represent densitometric analysis, data shown are mean ± SEM of 3 experiments performed in triplicates (*p ≤ 0.05; **p ≤ 0.01 vs controls).

also reduced in pBCEC. After a 24 h incubation period, Bex [100 nM] and Asx [10 nM] decreased intracellular cholesterol levels by 13 ± 2.5% and 28 ± 1.2% (Fig. 3G) (p ≤ 0.0001). These results together suggest that Asx and Bex promote release of cellular cholesterol and reduce endogenous cholesterol synthesis in pBCEC.

3.5. Asx and Bex upregulate LRP-1 along with Aβ uptake and transport in pBCEC

Aβ can be cleared from the brain via transcytosis across the BBB to the apical side [73]. We therefore studied the effect of both drugs on LRP-1, a multi-functional receptor known to be significantly involved in Aβ transport at the BBB [6,74]. qPCR experiments revealed that Bex dose-dependently up-regulated mRNA expression of *LRP-1* by 1.4 ± 0.31-fold (10 nM Bex) and 2.4 ± 0.29-fold (100 nM Bex), respectively (Fig. 4A) (p = 0.0291). In a similar manner, Asx increased *LRP-1* mRNA expression in pBCEC by 1.8 ± 0.10-fold (1 nM Asx) and 2 ± 0.18-fold (10 nM Asx) (Fig. 4B) (p = 0.0098).

We next investigated potential effects of both drugs on Aβ uptake and transcytosis in pBCEC. For uptake studies, cells pre-treated with vehicle control (0.5% ethanol), Bex [100 nM] or Asx [10 nM] for 24 h, were then incubated with Alexa Fluor 488 labeled $A\beta_{1-40}$ [0.5 μg/ml] for 2 h. Fluorimetric measurements revealed a decreased fluorescence intensity in the culture media of treated cells when compared to controls. This indicates that cellular uptake of Aβ was increased in a similar manner by Bex (20 ± 5.9%) and Asx (22 ± 3.3%) (Fig. 4C) (p = 0.0325). Alternatively, the relative uptake of $[^{125}I]$-$A\beta_{1-40}$ was increased by Bex (35 ± 11.7%) and Asx (55 ± 6.6%) (Fig. 4D) (p = 0.005). To further examine effects of Bex and Asx on Aβ transport, $[^{125}I]$-$A\beta_{1-40}$ was added to the basolateral compartment (mimicking brain parenchyma) of pBCEC cultured in transwell filter chambers, and Aβ transport to the apical compartment (mimicking the plasma environment) due to drug treatment was measured after 2 h. In line with the observed enhanced expression of *LRP-1*, Bex [100 nM] and Asx [10 nM] promoted transcytosis of Aβ across the in vitro BBB model by 1.2 ± 0.12-fold and by 1.5 ± 0.08-fold, respectively (Fig. 4E) (p = 0.0022).

3.6. Time-dependent and PPARα-/RXR-dependent effects of Asx and Bex on ABCA1, LRP-1, and APP/Aβ species in pBCEC

Time-dependent experiments were conducted to investigate the potential of Bex and Asx in addition to PA 542 and GW 6471 at different incubation periods to reveal whether expression of ABCA1, LRP-1, CTFs, ~80 KDa 6E10-reactive APP/Aβ species, as well as secreted sAPPα are mediated via RXR or PPARα.

Bex induced ABCA1 protein expression in a time-dependent manner up to 520% after 24 h (when compared to controls) via RXR pathway.

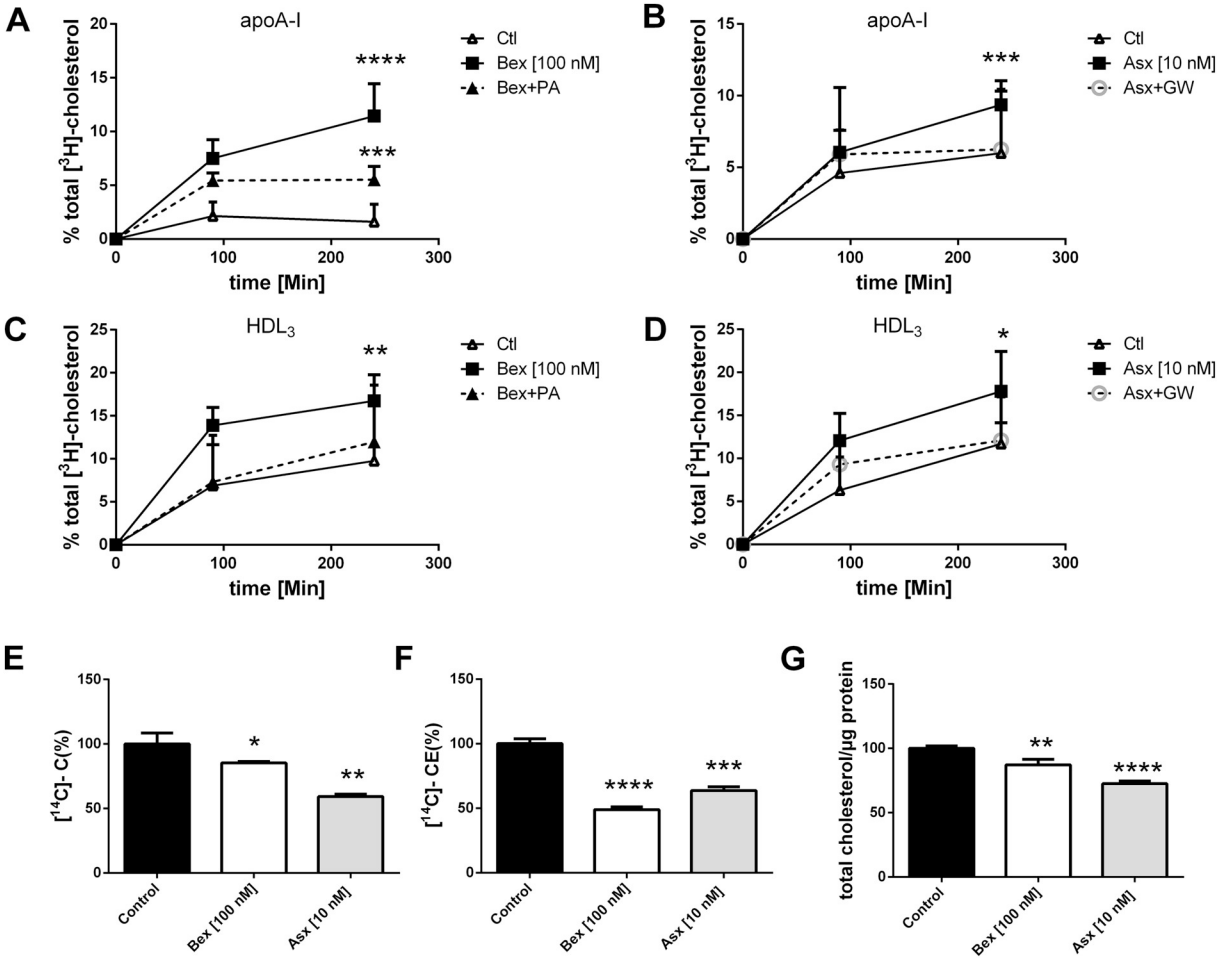

Fig. 3. Bex and Asx enhance time-dependent cholesterol release, in part via activation of RXR and PPARα, and reduce cholesterol levels and synthesis in pBCEC. (A–B) Cells cultured in 12-well plates were labeled with [^{3}H]-cholesterol for 24 h. Then cells were equilibrated for 16 h in serum-free medium, preincubated with RXR antagonist PA 452 [10 µM] or PPARα antagonist GW 6471 [10 µM] for 15 min, during incubation with 0.5% ethanol (vehicle control), Bex [100 nM], Asx [10 nM], Bex and PA 452, or Asx and GW 6471. Medium was changed and (A–B) apoA-I [10 µg/ml] or (C–D) HDL_3 [200 µg/ml] were added, and time-dependent cholesterol release to the culture medium was measured by β-counting. Data shown are mean ± SD of one representative experiment out of two (in presence of antagonists) or three (in absence of antagonists) performed in triplicates (*$p \leq 0.05$; **$p \leq 0.01$; ***$p \leq 0.001$; ****$p \leq 0.0001$ vs controls). (E–F) Cells were metabolically labeled for 24 h using cholesterol precursor [^{14}C]-acetate [2 µCi/ml] in the presence of 0.5% ethanol (vehicle control), Bex [100 nM] or Asx [10 nM]; unesterified [^{14}C]-cholesterol (E) and esterified [^{14}C]-cholesterol (F) was determined after TLC separation of Folch extracts and subsequent β-counting of individual bands cut out from TLC plates. Activity in cpm/well was normalized to mg cell protein and percentage of total activity was calculated (*$p \leq 0.05$; **$p \leq 0.01$; ***$p \leq 0.01$; ****$p \leq 0.0001$ vs controls). (G) Cells were treated for 24 h in the presence of 0.5% ethanol (control), Bex [100 nM] or Asx [10 nM] and cellular cholesterol content was measured enzymatically. Data represent mean ± SEM of 3 independent experiments performed in triplicates. *$p \leq 0.05$; **$p \leq 0.01$; ***$p \leq 0.001$ vs controls (**$p \leq 0.01$; ****$p \leq 0.0001$ vs controls).

Even after 8 h, treatment with RXR antagonist PA 542 in addition to Bex treatment suppressed expression of ABCA1 almost completely when compared to Bex treatment at 8 h (Fig. 5C).

Asx increased ABCA1 protein levels time-dependently up to 277% after 24 h (when compared to controls), whereas treatment of pBCEC with PPARα antagonist GW 6471 and Asx decreased expression of ABCA1 by 83% when compared to Asx treatment alone after 8 h (Fig. 5D).

Interestingly, expression of LRP-1 appeared also to be mediated through RXR activation, as treatment of pBCEC with Bex enhanced LRP-1 protein level time-dependently by 46% after 24 h (versus controls). However, treatment with PA 542 in addition to Bex reduced LRP-1 expression level by 58% (after 24 h) when compared to Bex treatment alone (Fig. 5E). In parallel, treatment of pBCEC with Asx enhanced LRP-1 levels by 63% after 24 h (when compared to controls), whereas treatment with GW 6471 in addition to Asx decreased LRP-1 levels by 59% (after 16 h) when compared to Asx treatment alone (Fig. 5F).

Bex also increased levels of CTF of APP in a time-dependent manner by 89% after 24 h (when compared to controls). Effects of Bex treatment on CTFs were also mediated by RXR since a 91% reduction in CTFs upon treatment with PA 542 in addition to Bex was observed when compared to Bex treatment of pBCEC after 8 h (Fig. 5G). In parallel, treatment of pBCEC with Asx increased CTF protein levels by 305% (when compared to controls after 16 h). However, treatment with GW 6471 in addition to Asx, decreased protein levels of CTF by 74% (when compared to Asx treatment after 16 h) (Fig. 5H). Interestingly, Bex significantly lowered 6E10-reactive APP/Aβ species even after 8 h by 82% (when compared to controls) (Fig. 5K). Asx further reduced also 6E10-reactive APP/Aβ species after 24 h by 82% (when compared to controls) (Fig. 5L). Bex induced sAPPα levels in a time-dependent manner by 110% after 24 h when compared to controls (Fig. 5I). In parallel, Asx enhanced sAPPα levels by 150% after 24 h (when compared to controls) (Fig. 5J). In contrast to CTFs, the expression of 6E10-reactive ~80 KDa APP/Aβ species and sAPPα was not reversed by the presence of either RXR or PPARα antagonists.

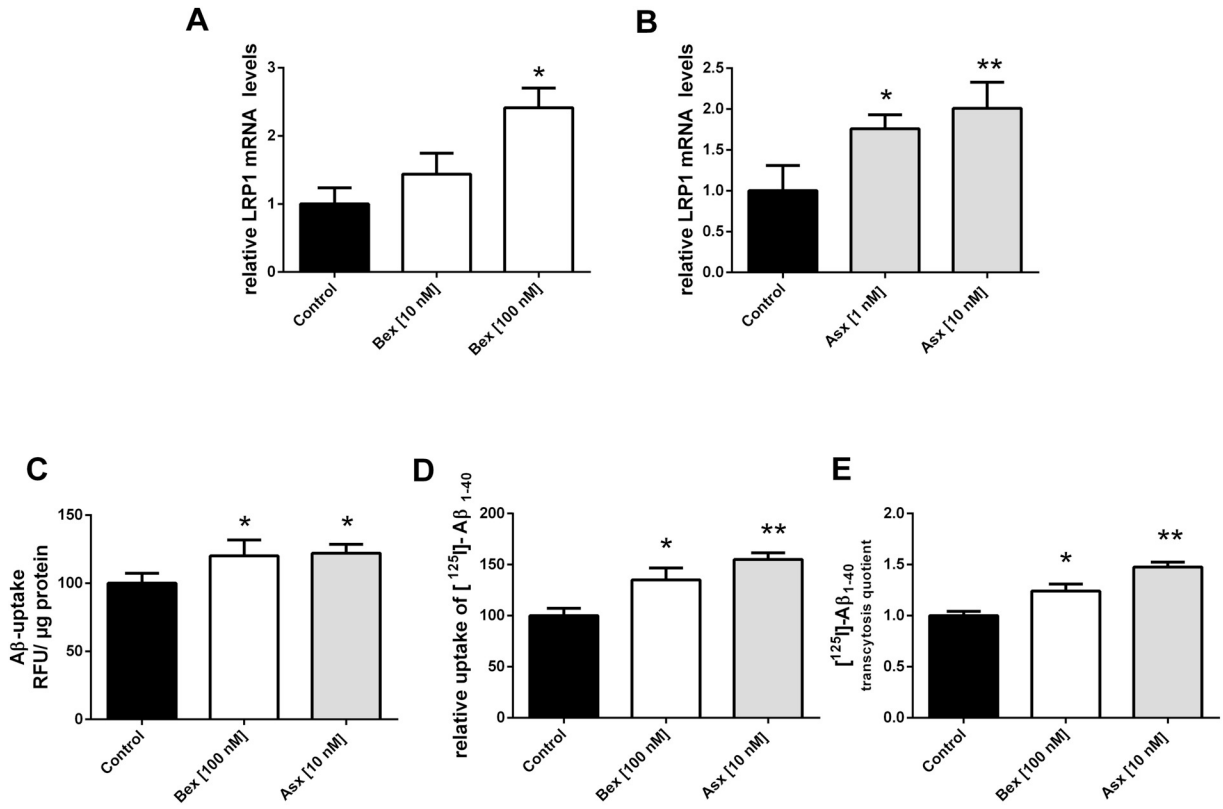

Fig. 4. Bex and Asx upregulate LRP-1 along with induced Aβ uptake and transport. (A–B) pBCEC cultured on 6-well plates were incubated with 0.5% ethanol (vehicle control), Bex [10 and 100 nM], or Asx [1 and 10 nM] for 24 h. Total RNA was isolated, reverse-transcribed, and subjected to qPCR using SYBR Green technology and HPRT1 as a house-keeping gene. The ΔΔCt method was applied to quantify relative mRNA expression levels. Data represent mean ± SEM from 3 experiments with different cell preparations each performed in triplicates (*p ≤ 0.05, **p ≤ 0.01 vs controls). (C) pBCEC were treated with 0.5% ethanol (control), Bex [100 nM] or Asx [10 nM] for 24 h. Cells were then washed and incubated with Alexa Fluor 488 labeled $Aβ_{1–40}$ [0.5 µg/ml] for 2 h, and fluorescence was measured at 490–525 nm using a Promega Glomax detection system (*p ≤ 0.05 vs controls. RFU: relative fluorescent units). (D) pBCEC were plated on transwells and treated with 0.5% ethanol (control), Bex [100 nM] or Asx [10 nM] for 24 h and tight junction formation was induced (overnight) by adding 550 nM hydrocortisone. TEER was measured using an Endohm ohmmeter. Aβ uptake assay was performed by adding 0.3 nM [^{125}I]-$Aβ_{1–40}$, and 100 nM [^{14}C]-sucrose as non diffusion control, to the basolateral compartment. Uptake of [^{125}I]-$Aβ_{1–40}$ was counted at 2 h from the apical compartment. TCA-precipitated proteins isolated from apical and basolateral media, were incubated on ice for 10 min and centrifuged at 10,000 ×*g* (10 min, 4 °C) and radioactivity associated to pellets was counted on a γ-counter. The supernatant was transferred to a new vial and the uptake of [^{125}I]-$Aβ_{1–40}$ was calculated as the percentage of cpm/mg cell protein in the pellet relative to the cpm/mg of supernatant. Data represent mean ± SEM from 3 experiments with different cell preparations each performed in triplicates (*p ≤ 0.05, **p ≤ 0.01 vs controls). (E) pBCEC were plated on transwells and treated with control (0.5% ethanol), Bex [100 nM] or Asx [10 nM] for 24 h, tight junction formation was induced (overnight) by adding 550 nM hydrocortisone. TEER was measured using an Endohm ohmmeter. Aβ transport assay was performed by adding 0.3 nM [^{125}I]-$Aβ_{1–40}$, and 100 nM [^{14}C]-sucrose as non diffusion control, to the basolateral compartment. Transport of [^{125}I]-$Aβ_{1–40}$ was counted at 2 h from the apical compartment and normalized to [^{14}C]-sucrose activity. Data represent mean ± SEM from 3 experiments performed in triplicates (*p ≤ 0.05, **p ≤ 0.01 vs controls).

3.7. LRP-1 silencing or ABCA1 inhibition reverses effects on APP processing/Aβ deposition in Bex- and Asx-treated pBCEC

Next, we investigated the effect of both drugs on LRP-1 protein level in non-silenced (NTC-)pBCEC and LRP-1-silenced pBCEC. Bex [100 nM] and Asx [10 nM] enhanced LRP-1 levels by 327% and 358%, respectively, when compared to controls (Fig. 6A). Silencing of LRP-1 was performed using a mix of previously validated short interfering sequences resulting in downregulation of endogenous LRP-1 on protein level by 61% in LRP-1-silenced Bex-treated [100 nM] pBCEC when compared to non-silenced Bex-treated cells, and by 69% in LRP-1-silenced Asx-treated [10 nM] pBCEC when compared to non-silenced Asx-treated cells (Fig. 6A). Strikingly, this reduction of LRP-1 levels modulated the cellular response to Aβ load (i.e. levels of 6E10-reactive APP/Aβ species) by 230% in LRP-1-silenced Bex-treated [100 nM] pBCEC when compared to non-silenced Bex-treated cells (Fig. 6B). In parallel, Aβ load was enhanced by 420% in LRP-1-silenced Asx-treated [10 nM] cells (when compared to non-silenced Asx-treated cells) (Fig. 6B).

We next analysed the effects of inhibiting ABCA1 activity with probucol (which inactivates ABCA1 in the plasma membrane [75]) on cellular APP processing products sAPPα and 6E10-reactive ~80 kDa band, and ABCA1 protein levels in pBCEC. Bex [100 nM] and Asx [10 nM] increased ABCA1 protein level by 236%, and 180%, respectively. Preincubation with probucol [10 µM] for 2 h and subsequent treatment with Bex [100 nM] or Asx [10 nM] for 24 h also decreased ABCA1 at protein level by 68% and 75% when compared to Bex- and Asx-treated cells in the absence of probucol (Fig. 6C). Similar to results shown in Figs. 1 and 5, treatment with Bex [100 nM] or Asx [10 nM] decreased intracellular 6E10-reactive ~80 kDa APP/Aβ species by 87% and 80%, respectively (Fig. 6D). In parallel, secreted sAPPα protein levels were increased by 150% (Bex) and 280% (Asx) when compared to controls (Fig. 6E). Furthermore, cellular treatment with probucol [10 µM] together with Bex [100 nM] or Asx [10 nM] for 24 h also decreased ABCA1 protein levels by 68% and 75% when compared to Bex- and Asx-treated cells in the absence of probucol (Fig. 6C). In parallel, 6E10-reactive ~80 kDa APP/Aβ species was markedly increased by 490% (Bex) and 480% (Asx) (Fig. 6D) while sAPPα protein levels were

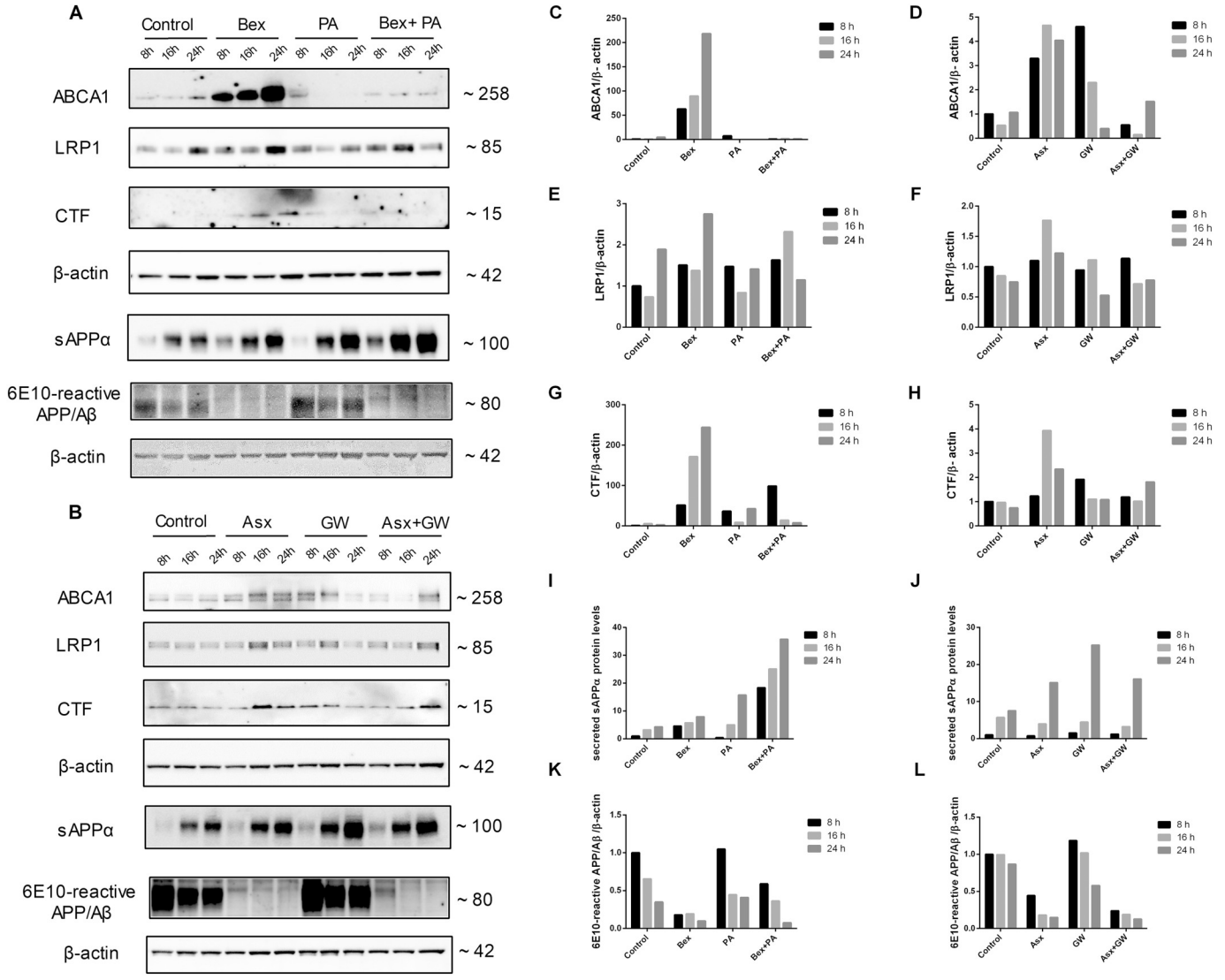

Fig. 5. Bex and Asx increase ABCA1 and LRP-1 protein expression in pBCEC, via nuclear receptor-dependent and independent mechanisms; in parallel APP processing products (CTFs and secreted sAPPα) are increased or decreased (~80 kDa 6E10-reactive APP/Aβ species) in a time-dependent manner. (A–H, K–L) pBCEC cultured on 6-well plates were pre-incubated in absence or presence of RXR antagonist PA 542 [10 μM] or PPARα antagonist GW 6471 [10 μM] for 15 min and treated with 0.5% ethanol (control), Bex [100 nM] or Asx [10 nM], Bex and PA 542, or Asx and GW 6471 for 8 h, 16 h, and 24 h. Proteins were extracted from cells, separated by SDS-PAGE, and levels of ABCA1, LRP-1, CTFs and 6E10-reactive APP/Aβ species (normalized to β-actin levels) were detected by immunoblot experiments. β-Actin was used as loading control. One representative blot out of 2 experiments is shown. The graphs represent densitometric evaluation of immunoreactive bands. (I–J) pBCEC cultured on 6-well plates were pre-incubated with PA 542 [10 μM] or GW 6471 [10 μM] for 15 min and treated with control (0.5% ethanol), Bex [100 nM] or Asx [10 nM], Bex and PA 542, or Asx and GW 6471 for 8 h, 16 h, and 24 h. Proteins (precipitated with TCA from supernatants) were separated by SDS-PAGE, and levels of secreted sAPPα (normalized to Ponceau stained bands) were detected by immunoblot experiments using 6E10 as primary antibody. One representative blot out of 2 experiments is shown. The graphs represent densitometric evaluation of immunoreactive bands.

reduced by 75% (Bex) and 99% (Asx), respectively (Fig. 6E).

3.8. Asx and Bex enhance LRP-1 and reduce BACE1 and Aβ oligomers level in mBCEC of 3xTg AD mice

Female 3xTg AD mice (32–49 weeks) and non-Tg mice (37–49 weeks) were gavaged for 6 days with either DMSO in corn oil (vehicle control), 100 mg/kg Bex or 80 mg/kg Asx in DMSO and corn oil. Hemispheres (2–3) obtained from different animals from individual groups were pooled and mBCEC were isolated.

Basically, significantly higher *APOE* mRNA expression levels were detected in mBCEC of all groups of 3xTg AD mice when compared to non-Tg mice: 3.8 ± 0.44-fold for vehicle-treated 3xTg AD relative to non-Tg vehicle-treated mice; 4.8 ± 0.54-fold for Bex-treated 3xTg AD versus Bex-treated non-Tg mice (Fig. 7A). Only Bex treatment further enhanced *APOE* levels in 3xTg AD mice by 1.4 ± 0.54-fold relative to vehicle-treated 3xTg AD mice and 2.9 ± 0.57-fold for Asx-treated 3xTg AD mice versus Asx-treated non-Tg mice. Two-way ANOVA revealed a significant effect of treatment ($p = 0.0244$). In contrast to *APOE*, *ABCA1* mRNA expression levels in mBCEC did not significantly differ in vehicle-treated 3xTg AD mice and vehicle-treated non-Tg mice (Fig. 7B). Isolated mBCEC of 3xTg AD mice treated with Bex, showed 2.2 ± 0.33-fold elevated *ABCA1* mRNA expression levels when compared to Bex-treated non-Tg mice. In mBCEC from Bex-treated 3xTg AD mice, *ABCA1* mRNA expression levels were elevated 1.7 ± 0.33-fold when compared to vehicle-treated 3xTg AD mice (Fig. 7B). Two-way ANOVA revealed a significant effect of treatment ($p = 0.0248$). On the other hand, in the Asx-treated group, no significant changes in *ABCA1* mRNA expression levels were detected when compared to the vehicle group (Fig. 7B).

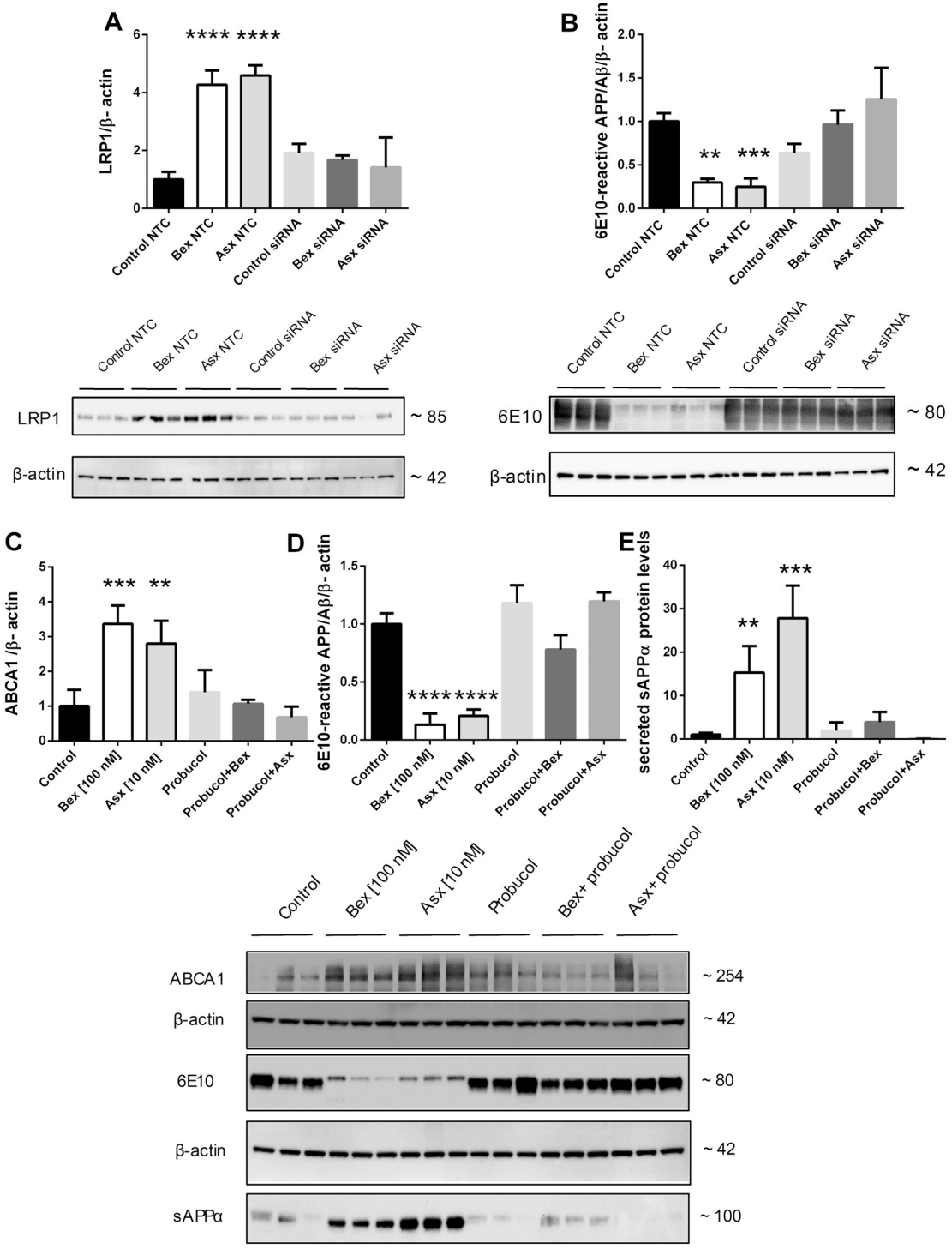

Fig. 6. Silencing of LRP-1 by RNA interference or inhibition of ABCA1 activity by probucol reverses effects on APP processing in Bex-/Asx-treated pBCEC. (A) pBCEC were cultured on 6-well plates and specific gene silencing was achieved by RNA interference using LRP-1 targeting siRNA, and NTC siRNA as control, for 48 h. After 24 h of silencing, cells were treated with Bex [100 nM] or Asx [10 nM] for 24 h. Proteins were extracted, separated by SDS-PAGE, and gene silencing efficiency was evaluated by immunoblot experiments using anti-LRP-1 as primary antibody. β-Actin was used as loading control (****$p \leq 0.0001$ vs controls). One representative blot out of 2 experiments is shown. (B), Levels of intracellular ~80 kDa APP/Aβ species (normalized to β-actin) were detected by immunoblot experiments using 6E10 as primary antibody. One representative blot out of 2 experiments is shown. The graphs represent densitometric evaluation of immunoreactive bands. (mean ± SD; **$p \leq 0.01$; ***$p \leq 0.001$ vs controls). (C–E) pBCEC cultured on 6-well plates were pre-incubated with specific ABCA1 inhibitor probucol [10 μM] for 30 min and treated with control (0.5% ethanol), Bex [100 nM] or Asx [10 nM], Bex and probucol, or Asx and probucol, for 24 h. Proteins were extracted from cells (precipitated with TCA from supernatants), separated by SDS-PAGE, and levels of intracellular ~80 kDa APP/Aβ species (normalized to β-actin) and secreted sAPPα (normalized to Ponceau stained bands) were detected by immunoblot experiments using 6E10 as primary antibody. One representative blot out of 2 experiments is shown. The graphs represent densitometric evaluation of immunoreactive bands. (mean ± SD; **$p \leq 0.01$; ***$p \leq 0.001$; ****$p \leq 0.0001$ vs controls).

BACE1 mRNA expression levels were elevated by 2.0 ± 0.4-fold in mBCEC isolated from vehicle-treated 3xTg AD compared to vehicle-treated non-Tg mice (Fig. 7C). However, gavaging 3xTg AD mice with Bex or Asx reduced *BACE1* mRNA expression levels in mBCEC by 62 ± 1.1% and 71 ± 0.7% (Fig. 7C), when compared to mBCEC obtained from vehicle-treated 3xTg AD mice. Two-way ANOVA revealed a significant effect of treatments in 3xTg AD mice (p = 0.0272). *BACE1* mRNA expression levels were not affected by any treatment in mBCEC from non-Tg mice (Fig. 7C).

We further show that Bex and Asx considerably enhanced *LRP-1* mRNA levels by 3.5 ± 0.31-fold 2.4 ± 1.3-fold in mBCEC isolated from 3xTg AD mice when compared to vehicle-treated 3xTg AD mice

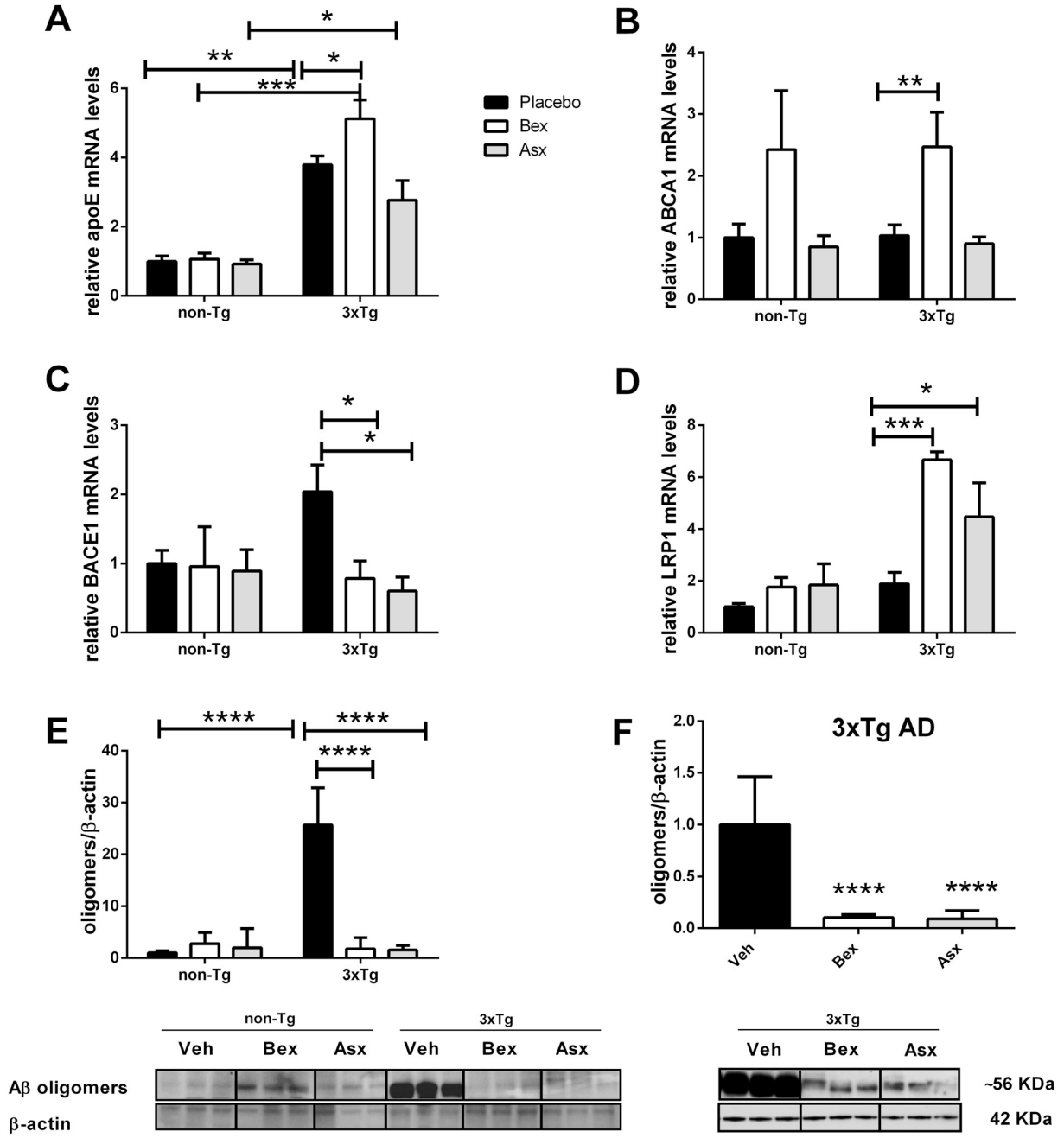

Fig. 7. Asx and Bex enhance *LRP-1* and reverse *BACE1* and Aβ oligomer levels in mBCEC of 3xTg AD as compared to non-TG mice. (A–D) *study I*: Female 3xTg AD mice and C57BL/6 (non-Tg) mice were gavaged for 6 days vehicle (10% DMSO and corn oil) (n = 10), Bex (n = 9) and Asx (n = 8) and non-Tg mice, vehicle (n = 5), Bex (n = 6) and Asx (n = 7). Two to three hemispheres were pooled to isolate mBCEC RNA was isolated and reverse-transcribed to cDNA. qPCR analysis was performed using the ΔΔCt method and HPRT1 as housekeeping gene. Data were normalized to vehicle-treated non-Tg mice. All data represent mean ± SEM from 3 to 4 samples performed in triplicates (*p ≤ 0.05; **p ≤ 0.01; ***p ≤ 0.001 vs controls). (E) *study I*: Female 3xTg AD mice were gavaged for 6 days with DMSO in corn oil as vehicle/control (n = 10), Bex (n = 9), or Asx (n = 8) in DMSO and corn oil and non-Tg mice, vehicle (n = 5), Bex (n = 6) and Asx (n = 7). Two to three hemispheres were pooled to isolate mBCEC. Cellular proteins were extracted, separated by SDS-PAGE and Aβ oligomers level were detected by immunoblot experiments using polyclonal anti-amyloid oligomer antibody A11 and normalized to β-actin levels. Data shown are mean ± SEM of 3 pooled samples (****p ≤ 0.0001 vs controls). (F) *study II*: Female 3xTg AD mice were gavaged for 6 days with DMSO in corn oil as vehicle/control (n = 8), Bex (n = 6), or Asx (n = 8) in DMSO and corn oil. Two hemispheres were pooled to isolate mBCEC. Cellular proteins were extracted, separated by SDS-PAGE and Aβ oligomers level were detected by immunoblot experiments using polyclonal anti-amyloid oligomer antibody A11. Immunoreactive bands were normalized to β-actin. Data shown are mean ± SEM of 3 to 4 pooled samples (****p ≤ 0.0001 vs controls).

(Fig. 7D). Two-way ANOVA revealed a significant effect of treatment ($p = 0.0072$). In *study I*, mBCECs were homogenized and aliquots of protein lysates were subjected to immunoblot experiments to follow expression of Aβ oligomers. Basically, a distinct immunoreactive ~56 kDa band (representing murine Aβ oligomers, [76]) was observed in mBCEC protein lysates. Strikingly, Aβ oligomers almost disappeared in mBCEC from 3xTg AD mice when treated with either Bex (reduction by 93 ± 30.3%) or Asx (reduction by 94 ± 12.6%) (Fig. 7E) when compared to vehicle-treated 3xTg AD mice. Two-way ANOVA revealed a significant effect of treatment ($p \leq 0.0001$).

In *study II*, aged female 3xTg AD mice (68–92 weeks) were gavaged for 6 days with DMSO in corn oil as vehicle/control, 100 mg/kg Bex, or 80 mg/kg Asx in DMSO and corn oil. For isolation of mBCEC, 2–3 hemispheres were pooled. mBCECs were subjected to immunoblot experiments to follow expression of Aβ oligomers. Basically, a distinct immunoreactive ~56 kDa band (indicative for Aβ oligomers) was observed in mBCEC protein lysates similar to *study I*. Strikingly, Aβ oligomers almost disappeared in mBCEC from 3xTg AD mice when treated with either Bex (reduction by 89 ± 11.9%) or Asx (reduction by 90 ± 20.3%) (Fig. 7F) when compared to vehicle-treated 3xTg AD mice. Two-way ANOVA revealed a significant effect of treatment ($p \leq 0.0001$).

Of note, treatment of mice with Bex elevated plasma levels of cholesterol (Supplementary Fig. IVA, IVD) ($p \leq 0.0001$) and triglycerides (Supplementary Fig. IVB [$p = 0.0004$], IVE [$p = 0.0155$]), data in line with previous findings [77]. However, no significant changes in plasma cholesterol or triglycerides levels due to Asx treatment could be observed. Furthermore, significant weight loss (Supplementary Fig. IVC [$p \leq 0.0001$], IVF [$p \leq 0.0001$]), and hepatomegaly (data not shown) became apparent in 3xTg AD mice subjected to Bex treatment, data that parallel previous findings [78]. In contrast, neither side effects nor body weight changes were observed in mice following Asx treatment; findings in line with a previous report [79].

3.9. Immunoblotting of Aβ monomers and oligomers in soluble (DEA) and insoluble (FA) fractions of mice cortical brain

We next performed immunoblotting experiments for Aβ in the DEA soluble and FA insoluble fractions from mouse brain tissue extracts, using 6E10 as primary antibody that recognizes all Aβ species including monomeric and oligomeric Aβ. The intensity of monomeric and oligomeric Aβ bands were increased in brain samples from vehicle-treated 3xTg AD compared to vehicle-treated non-Tg mice in both fractions.

Six distinct bands, similar as shown by Manczak and coworkers [80] were detected (Fig. 8B); one with ~110 kDa representing APP and the other band with ~56 kDa representing Aβ oligomers [81], in addition to (~26 kDa), trimers/CTF (~13 kDa), dimers (~8 kDa) and the monomeric band (~4 kDa).

Interestingly, in the DEA fraction, a clear reduction in Aβ monomers and trimeric Aβ/CTFβ (~13 kDa) [81] was observed in Bex- and Asx-treated 3xTg AD mice when compared to vehicle-treated 3xTg AD mice (Fig. 8B). In addition, the ~56 putative oligomeric Aβ was also decreased in both Bex- and Asx-treated 3xTg AD mice when compared to vehicle-treated 3xTg AD mice (Fig. 8B). The ~56 kDa band has been previously reported in brain soluble extracts from AD patients [82] and in brain tissues from APP transgenic mice [83].

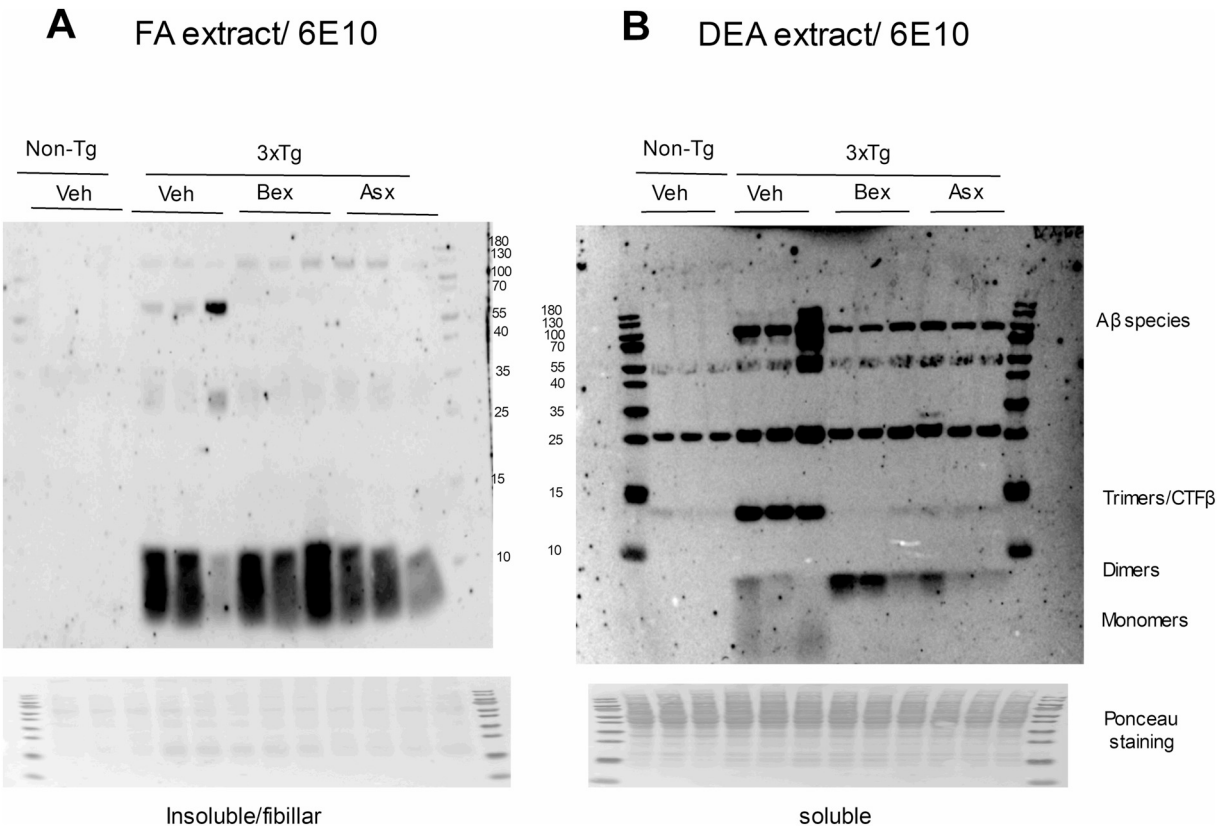

Fig. 8. Bex and Asx treatment reduce Aβ species in brain DEA and FA fractions in 3xTg AD mice. Female 3xTg AD mice and C57BL/6 (non-Tg) mice were gavaged for 6 days vehicle (10% DMSO and corn oil) (n = 10), Bex (n = 9) and Asx (n = 8) and non-Tg mice, vehicle (n = 5), Bex (n = 6) and Asx (n = 7). One brain hemisphere of each animal was mechanically homogenized in tissue homogenization buffer and sequential extractions of both insoluble FA and soluble DEA fractions were performed as described in Materials and Methods. Proteins were separated by SDS-PAGE and Aβ species and monomers were detected by immunoblot experiments using 6E10 as primary antibody. Ponceau staining was used as loading control.

The high molecular weight Aβ species (~30 and ~60 kDa) detected in the FA fraction were also decreased by Bex- and Asx-treatment in 3xTg AD when compared to vehicle-treated 3xTg AD mice. Interestingly, no significant changes were observed in monomeric Aβ (Fig. 8A).

3.10. Asx and Bex reduce Aβ load in cerebrovascular endothelial cells and brain parenchyma of 3xTg AD mice

Immunofluorescence double staining of snap frozen 18 μm sections of brains derived from female 3xTg AD mice (68–92 weeks), that normally express more pronounced Aβ deposits than younger 3xTg AD mice, was performed for vWF (an endothelial cell marker) and 6E10 staining, detecting the N-terminal portion (amino acid residues 1–16) of Aβ (Fig. 9A). Colocalization of vWF and Aβ (using anti-β-Amyloid 6E10 as primary antibody) became apparent. Asx-treated mice showed a diffused form of Aβ deposition in cerebrovascular cells (Fig. 9Ak) while mice treated with Bex showed a reduced number of Aβ epitopes (Fig. 9Ag) when compared to vehicle-treated mice (Fig. 9Ac). In line with data obtained from immunoblot experiments (Fig. 7E, F), less 6E10-reactive staining became visible in cerebrovascular cells when treated with Bex and Asx (Fig. 9Ah, Al), respectively, when compared to vehicle controls (Fig. 9Ad).

Using either the Aβ oligomer-specific antibody A11 or anti-β-Amyloid 6E10 antibody on snap-frozen brain sections from female 3xTg AD mice (68–92 weeks), a pronounced reduction of immunofluorescence of Aβ/oligomers was observed on sections from mice treated with Bex (Fig. 9Bd, Be) or Asx (Fig. 9Bg, Bh) when compared to vehicle-treated 3xTg AD mice (Fig. 9Ba, Bb).

4. Discussion

During the present study, we identified effects of the PPARα agonist Asx and the RXR agonist Bex on pathways of APP processing, Aβ transfer across the BBB, and on pathways crucial for maintaining cholesterol homeostasis in cerebrovascular endothelial cells mimicking the BBB. The major findings are (i) that both drugs exert profound and similar effects on APP processing and Aβ clearance in BCEC, (ii) the major targets identified in BCEC (in vitro and in vivo) and in total brain tissue are *BACE1*, *ABCA1* and *LRP-1*, and (iii) a link between improved cellular cholesterol homeostasis in BCEC with reduced Aβ load appears evident.

Importantly, Bex has been found to reduce Aβ load and/or cognitive impairment in mouse models of AD [53,84–87] as proposed by its RXR activating properties [88]. However, to our knowledge, effects of Bex have only been addressed to some extent [89,90] and those of Asx have not yet been investigated in vitro or in vivo as a potent modulator of BBB function in AD. During initial experiments we examined whether Asx and Bex may regulate APP processing enzymes, amyloidogenic Aβ oligomers, and non-amyloidogenic APP product sAPPα in pBCEC, a cellular in vitro system mimicking the BBB and known to promote APP/Aβ processing and transport [34,35]. In response to either Asx or Bex treatment, dose-dependently increased mRNA expression levels of *APP*, α secretase *ADAM10* and elevated sAPPα protein levels were observed in pBCEC. In parallel, a prominent 6E10-reactive intracellular ~80 kDa APP/Aβ species almost disappeared in pBCEC with the higher doses of Asx/Bex used. Absence of cross-reactivity with anti-C-terminal APP antibody was confirmed (data not shown), however, the exact nature of the APP processing product remains to be established in future experiments. Furthermore, a decrease in β-secretase *BACE1* on mRNA expression and activity levels, as well as reduced Aβ oligomers in pBCEC were observed. Taken together, it seems that Asx and Bex direct APP processing in pBCEC towards the non-amyloidogenic pathway.

Interestingly, ADAM10 levels were found to be reduced in elderly AD patients when compared to elderly non-AD subjects [91]. Stimulating the non-amyloidogenic route or preventing the generation of Aβ peptide through promoting α-secretase ADAM10 as optional therapeutic treatments has been investigated [92]. Cholesterol reduction may enhance α-secretase activity [93] and it appears that cholesterol levels are linked to β-amyloidogenesis and cytotoxicity of Aβ [94]. For example, altered cellular cholesterol homeostasis does interfere with APP metabolism, since cholesterol-rich lipid rafts located at cellular membrane have been proposed as the site for proteolytic processing of APP [95].

We here demonstrate that cellular cholesterol homeostasis is altered in pBCEC in response to Asx or Bex. We further show that mRNA and protein expression levels of ABCA1 are upregulated after treatment with Bex or Asx in pBCEC in a dose- and time-dependent manner. Since LXRs (as do PPARs) heterodimerize with RXR to become active, RXR activation may enhance transcription of LXR and PPAR target genes. We previously reported that in addition to LXR agonists, PPAR agonists enhanced expression of ABCA1 and apoA-I in pBCEC [39]. Thus, a likely explanation for up-regulated ABCA1 and apoA-I/apoE expression by Asx and/or Bex, is that both drugs may act as potent PPARα or RXR agonist. The higher doses of Bex [100 nM] and Asx [10 nM] in absence and presence of RXR or PPARα antagonists were employed to study time-dependent effects on ABCA1 expression and cholesterol efflux from pBCEC. Asx and Bex promoted apoA-I- and HDL-mediated [^{3}H]-cholesterol efflux from pBCEC, an observation in line with up-regulation of ABCA1 and ABCG1, respectively. Nuclear receptor antagonists partially reversed up-regulation of ABCA1 by Asx/Bex treatment, which was also reflected by reduced cholesterol efflux. Thus, RXR and PPARα seem to play important roles in the regulation of cholesterol homeostasis in pBCEC in line with earlier observations by our group [39] and similar to cortical astrocytes [100].

ApoA-I (involved in cholesterol efflux) was up regulated after treatment with Bex in pBCEC. pBCEC do not express apoE, however, do synthesize and secrete apoA-I [37]. In contrast, mBCEC express apoE but no apoA-I (unpublished observations). We further observed that Bex significantly elevated *APOE* and *ABCA1* expression levels in mBCEC while Asx elevated mRNA expression levels of *ABCA1* in pBCEC. ApoE, a major cholesterol carrier in the brain (i) promotes lipid transport, (ii) can bind to cell-surface receptors to deliver lipids and (iii) also binds to Aβ apparently regulating its clearance [96–99]. Immunoblot experiments confirmed an increase in apoA-I on protein level in pBCEC when treated with Bex. While in animal studies a concentration of 100 mg/kg Bex markedly increased expression levels of *APOE* and *ABCA1* in BCEC, treatment with 80 mg/kg of Asx did not significantly alter mRNA expression levels of *APOE* and *ABCA1*.

We obtained strong evidence for a requirement of active ABCA1 to affect APP processing and Aβ load in pBCEC, since inhibiting ABCA1 by probucol fully reversed effects of Bex and Asx by increasing Aβ loads in pBCEC and reducing cellular release of non-amyloidogenic sAPPα. Importantly, and in line with our findings (with Bex), the presence of ABCA1 and ABCA1-induced lipidation of apoE was reported to be necessary for the ability of Bex to clear hippocampal soluble Aβ and to ameliorate cognitive deficits in APP/PS1 mice [87].

Cellular cholesterol efflux promoted by the apoA-I- or apoE/ABCA1-mediated pathway has also been reported to alter secreted Aβ levels [97]. Thus, increased ABCA1 expression suppressed Aβ levels in an AD mouse model [100] and ABCA1 deficiency led to higher Aβ deposition [101]. Importantly, enhanced ABCA1 expression and induction of cholesterol efflux by Bex treatment has been reported in an in vitro model of human BCEC [90] and cholesterol efflux from macrophages has further been found to be enhanced by Asx treatment [102]. Previous studies have shown that dietary supplementation with Asx raises serum levels of HDL-cholesterol in humans [103,104], an observation that may reflect increased cellular cholesterol efflux. It is also known that Aβ assembly to fibrils can be inhibited by the presence of HDL-like particles [105], further supporting the protective function(s) of HDL. Here, Asx and Bex (i) enhanced cholesterol release and (ii) reduced cholesterol biosynthesis and esterification from [^{14}C]-acetate in pBCEC.

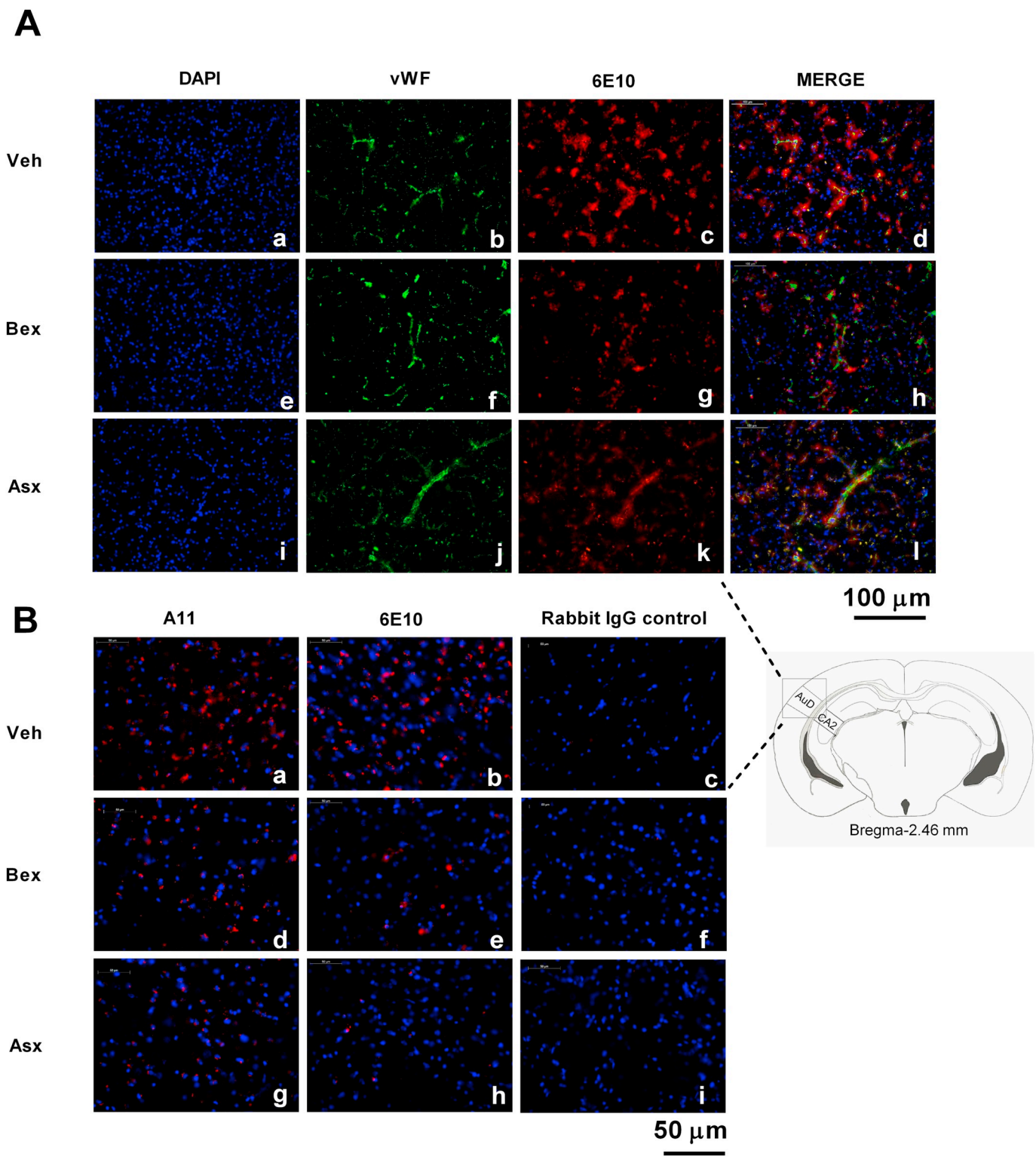

Fig. 9. Bex and Asx reduce Aβ specific staining in cerebrovascular endothelial cells and in brain parenchyma of aged 3xTg AD mice. (A) Immunofluorescence double staining was performed on snap-frozen 18 μm sections of mouse brains obtained from untreated and Bex- or Asx-treated (as described in Materials and Methods Section 2.17) female 3xTg AD mice by using anti-Aβ antibody (6E10) at 5.0 μg/ml (c,g,k) and rabbit anti-human-vWF at 0.16 μg/ml (b,f,j) for 1 h. Sections were washed with TBST and secondary antibodies, i.e. goat anti-rabbit Cy-3 (red, 1.88 μg/ml) and donkey anti-rabbit Dylight 488 (green, 1.66 μg/ml) were applied for 30 min. Sections were rinsed with TBST and DAPI was added to the slides for 20 min as a nuclei counter stain (blue). Images are from auditory cortex dorsal part. Veh (vehicle). (B) Immunofluorescence staining was performed on snap-frozen mouse brain 18 μm sections by using polyclonal anti-amyloid oligomer antibody A11 (AB9234, 8 μg/ml) (a,d,g) and anti-Aβ antibody 6E10 (SIG-39320, 5 μg/ml) (b,e,h) for 1 h. Slides were washed with TBST and goat anti-rabbit Cy-3 (red, 1.88 μg/ml) was used as a secondary antibody (30 min). Sections were rinsed again with TBST and DAPI was added to the slides for 20 min as a nuclei counter stain (blue). Non-immune rabbit or mouse IgG was used as negative control (c,f,i). Images are from auditory cortex dorsal part. (For interpretation of the references to colour in this figure legend, the reader is referred to the web version of this article.)

Taken together, both drugs are apparent modulators of cellular cholesterol and Aβ homeostasis; furthermore, both drugs control cholesterol efflux by regulating expression of ABCA1 and by reducing cholesterol ester content and cholesterol biosynthesis in pBCEC. Our in vitro data suggest that Asx and Bex are cytoprotective by reducing cholesterol and Aβ. Our data further suggest that decreased de novo cholesterol synthesis drives a non-amyloidogenic pBCEC phenotype, potentially in response to a reshuffling of different cellular cholesterol pools.

By investigating the effects of Asx and/or Bex on in vitro uptake and transport of $A\beta_{1–40}$ across polarized cerebrovascular endothelial cells, we here demonstrate that Asx and Bex promote transcytosis of [^{125}I]-$A\beta_{1–40}$ from the 'brain' to the 'plasma' compartment. Importantly, we found mRNA and protein expression levels of LRP-1 at the BBB, that is involved in the uptake, transport and clearance [6] of amyloid fragments, significantly up-regulated in response to Asx and Bex in pBCEC. The role of LRP-1 in the pathogenesis of the AD [106], in particular brain endothelial LRP-1, has been extensively investigated as a potential target for AD therapy [107]. Monomeric $A\beta_{1–40}$ can bind to special domains of LRP-1 [108]; in parallel oligomeric or aggregated Aβ is also a poor ligand for LRP-1 [108,109]. The important function of cerebrovascular LRP-1 for Aβ elimination from the brain has been recently proven via tamoxifen-inducible deletion of *LRP-1* in the 5xFAD mouse model of AD within brain endothelial cells; such deletion resulted in reduced plasma Aβ levels but elevated soluble Aβ in the brain [6].

We here confirmed that LRP-1 mediates brain Aβ clearance and impacts amyloid load in pBCEC in vitro. Our results further demonstrate that a reduction of Aβ species by Bex and Asx involves LRP-1, as the silencing of LRP-1 did not diminish intracellular Aβ load in Bex- and Asx-treated pBCEC.

Using forebrain neuron-specific LRP-1$^{-/-}$ mice, Tachibana and coworkers [78] recently reported that beneficial effects of Bex on synaptic integrity depend on the presence of neuronal LRP-1, while ABCA1 and apoE levels in the brain were also increased by Bex in both nLRP-1$^{-/-}$ and wild-type mice. Neuroinflammation was suppressed by Asx through promoting M2 microglia polarization in an LRP-1-dependent manner in BV2 cells stimulated with lipopolysaccharide [110], emphasizing a potential anti-inflammatory therapeutic effect of Asx.

In vivo, we here confirm that treatment with Bex enhanced *ABCA1* and *apoE* expression levels, and Bex and Asx enhanced *LRP-1* in mBCEC of 3xTg AD mice.

Intriguingly, and coherent with our in vitro results obtained from pBCEC, treatment with either drug diminished BACE1 expression in mBCEC. Significantly lower cerebral Aβ levels in mice were reported by applying designed BACE1 peptide inhibitors [111] and BACE inhibitors were proposed potential potent therapeutics to reduce Aβ levels [112]. Reversed Aβ deposition and improved cognitive function have recently been demonstrated in BACE1 conditional knockout mice [16]. Interestingly, a direct albeit low binding efficacy of Bex to BACE1 was reported [113]. It has further been suggested that increased cellular cholesterol levels (in Niemann-Pick disease, type C1-deficient cells) may drive amyloidogenic APP processing by altering the endocytic trafficking of APP and BACE1 [114] and cholesterol depletion corrected APP and BACE1 mistrafficking. Thus, a reduction of cellular cholesterol mediated by Asx or Bex per se, as observed in the present study, might reduce BACE1 recruitment to lipid rafts thereby reducing Aβ production.

We further investigated the amyloid burden in brain soluble and insoluble Aβ fractions of 3xTg AD mice and non-Tg mice by immunoblotting. A pronounced clearance/reduction of monomeric, trimeric/CTFβ and less pronounced reduction in putative oligomers was detected in soluble Aβ fractions obtained from brains of Bex- and Asx-treated 3xTg AD mice (when compared to vehicle-treated 3xTg AD). No significant reduction of monomeric Aβ was detected in the insoluble fractions. Our data on Bex effects overall are in line with those by Corona and coworkers [87], reporting reduced levels of soluble Aβ

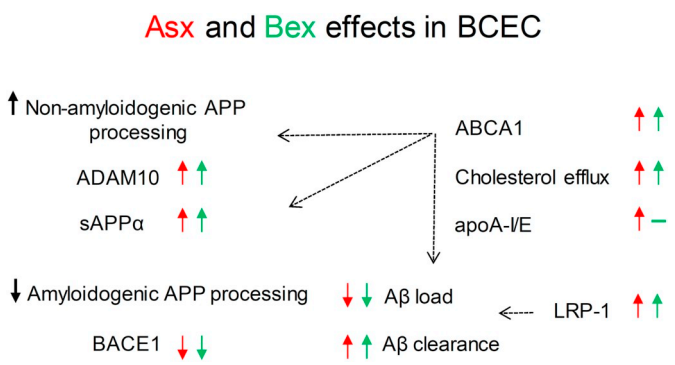

Fig. 10. Scheme depicting beneficial effects of Asx and Bex in brain capillary endothelial cells. Asx (red) and Bex (green) reduce cholesterol biosynthesis and esterification but promote cholesterol efflux by elevating ABCA1 and apoA-I/E levels. ABCA1 plays a crucial role in improving BCEC APP/Aβ homeostasis, as inhibition of ABCA1 retains Aβ load in the cells and decreases secretion of beneficial, non-amyloidogenic sAPPα. Asx and Bex promote the non-amyloidogenic route of APP processing, represented by elevated *ADAM10* and sAPPα levels. In parallel, amyloidogenic APP processing is diminished by reduced BACE1 activity. Consequently, less Aβ is produced by BCEC. In parallel, LRP-1 levels at the BBB are increased likely contributing to enhanced Aβ clearance by accelerating Aβ uptake and transcytosis across at the BBB, in turn, reducing Aβ/oligomers in the cerebrovasculature and in the brain. (For interpretation of the references to colour in this figure legend, the reader is referred to the web version of this article.)

1–40 and 1–42 in the hippocampus of Bex-treated ABCA1 wild-type but not ABCA1 knock-out APP/PS1 mice. In contrast, insoluble levels of Aβ and plaque loads were also unaffected by Bex in that study.

Brain sections of Bex- and Asx-treated 3xTg AD mice were stained histologically and neither morphological changes nor shrunken cell bodies or dark cytoplasm were observed; this is indicative for that neuronal integrity was maintained (Supplementary Fig. V).

However, it is important to note that in sharp contrast to Asx and as also pointed out by others [78], Bex administration may promote adverse side effects, such as hepatomegaly and significant weight loss. Medical application has also been suggested to be reconsidered since Bex may modulate serum lipid that may increase the risk of stroke and heart attack [115]. In contrast, Asx might act as a potential therapeutic drug due to its safety and health-promoting effects.

Based on our results (Fig. 10), we suggest that Asx and Bex increase the clearance of Aβ from the brain by increasing transcription of LRP-1 and ABCA1 in BCEC of 3xTg AD brains. Bex and Asx affect not only the clearance but also generation of Aβ since both drugs shift APP processing towards the non-amyloidogenic pathway by reducing BACE-1 (activity) and Aβ/oligomers in mBCEC and in deeper regions of the brain.

Conflicts of interest

The authors declare that there are no conflicts of interest associated with this study.

Transparency document

The Transparency document associated with this article can be found in the online version.

Acknowledgments

This work was supported by the Austrian Science Fund, grants P24783-B19 (to U.P.), and W1226-B18 (to E.F.D., J.T., F.M., and U.P.; Doctoral College of Metabolic and Cardiovascular Disease, DK-MCD, co-funded by the Medical University of Graz). F.M. is also grateful to the

Austrian Science Fund for grants P23490-B20, P29262, P24381, P29203, P27893, I1000, and “SFB Lipotox” (F3012), as well as the Bundesministerium für Wissenschaft, Forschung und Wirtschaft, and the Karl-Franzens University of Graz for grant “Unkonventionelle Forschung”. We acknowledge support from NAWI Graz and the BioTechMed-Graz flagship project “EPIAge”. Additional support was provided by Fundació La Marató de TV3 grant 2014-0930 (to A.C.) and an FPU fellowship from Ministerio de Economía y Competitividad (MEC) (to C.dD) and the Austrian National Bank (OeNB, 17600 to E.M.).

Appendix A. Supplementary data

Supplementary data to this article can be found online at https://doi.org/10.1016/j.dummy.2019.01.002.

References

[1] K.E. MacDuffie, A.S. Atkins, K.E. Flegal, C.M. Clark, P.A. Reuter-Lorenz, Memory distortion in Alzheimer's disease: deficient monitoring of short- and long-term memory, Neuropsychology. 26 (2012) 509–516, https://doi.org/10.1037/a0028684.

[2] R. Anand, K.D. Gill, A.A. Mahdi, Therapeutics of Alzheimer's disease: past, present and future, Neuropharmacology. 76 Pt A (2014) 27–50, https://doi.org/10.1016/j.neuropharm.2013.07.004.

[3] G.G. Glenner, C.W. Wong, Alzheimer's disease: initial report of the purification and characterization of a novel cerebrovascular amyloid protein, Biochem. Biophys. Res. Commun. 120 (1984) 885–890.

[4] I. Grundke-Iqbal, K. Iqbal, Y.C. Tung, M. Quinlan, H.M. Wisniewski, L.I. Binder, Abnormal phosphorylation of the microtubule-associated protein tau (tau) in Alzheimer cytoskeletal pathology, Proc. Natl. Acad. Sci. U. S. A. 83 (1986) 4913–4917.

[5] R. Deane, R.D. Bell, A. Sagare, B.V. Zlokovic, Clearance of amyloid-beta peptide across the blood-brain barrier: implication for therapies in Alzheimer's disease, CNS Neurol. Disord. Drug Targets. 8 (2009) 16–30.

[6] S.E. Storck, S. Meister, J. Nahrath, J.N. Meißner, N. Schubert, A. Di Spiezio, S. Baches, R.E. Vandenbroucke, Y. Bouter, I. Prikulis, C. Korth, S. Weggen, A. Heimann, M. Schwaninger, T.A. Bayer, C.U. Pietrzik, Endothelial LRP1 transports amyloid-β(1-42) across the blood-brain barrier, J. Clin. Invest. 126 (2016) 123–136, https://doi.org/10.1172/JCI81108.

[7] N.M. de Wit, G. Kooij, H.E. de Vries, In vitro and ex vivo model systems to measure ABC transporter activity at the blood-brain barrier, Curr. Pharm. Des. 22 (2016) 5768–5773.

[8] M. Yamada, Cerebral amyloid angiopathy: emerging concepts, J. Stroke. 17 (2015) 17–30, https://doi.org/10.5853/jos.2015.17.1.17.

[9] E.G. Stopa, P. Butala, S. Salloway, C.E. Johanson, L. Gonzalez, R. Tavares, V. Hovanesian, C.M. Hulette, M.P. Vitek, R.A. Cohen, Cerebral cortical arteriolar angiopathy, vascular beta-amyloid, smooth muscle actin, Braak stage, and APOE genotype, Stroke. 39 (2008) 814–821, https://doi.org/10.1161/STROKEAHA.107.493429.

[10] X.-Z. Yuan, S. Sun, C.-C. Tan, J.-T. Yu, L. Tan, The role of ADAM10 in Alzheimer's disease, J. Alzheimers Dis. JAD. 58 (2017) 303–322, https://doi.org/10.3233/JAD-170061.

[11] R. Coronel, A. Bernabeu-Zornoza, C. Palmer, M. Muñiz-Moreno, A. Zambrano, E. Cano, I. Liste, Role of amyloid precursor protein (APP) and its derivatives in the biology and cell fate specification of neural stem cells, Mol. Neurobiol. 55 (2018) 7107–7117, https://doi.org/10.1007/s12035-018-0914-2.

[12] R. Vassar, BACE1: the beta-secretase enzyme in Alzheimer's disease, J. Mol. Neurosci. MN. 23 (2004) 105–114, https://doi.org/10.1385/JMN:23:1-2:105.

[13] J. Zhao, Y. Fu, M. Yasvoina, P. Shao, B. Hitt, T. O'Connor, S. Logan, E. Maus, M. Citron, R. Berry, L. Binder, R. Vassar, Beta-site amyloid precursor protein cleaving enzyme 1 levels become elevated in neurons around amyloid plaques: implications for Alzheimer's disease pathogenesis, J. Neurosci. 27 (2007) 3639–3649, https://doi.org/10.1523/JNEUROSCI.4396-06.2007.

[14] S. Crunkhorn, Alzheimer disease: BACE1 inhibitor reduces β-amyloid production in humans, Nat. Rev. Drug Discov. 16 (2016) 18, https://doi.org/10.1038/nrd.2016.271.

[15] F. Peters, H. Salihoglu, E. Rodrigues, E. Herzog, T. Blume, S. Filser, M. Dorostkar, D.R. Shimshek, N. Brose, U. Neumann, J. Herms, BACE1 inhibition more effectively suppresses initiation than progression of β-amyloid pathology, Acta Neuropathol. (Berl.). (2018). doi:10.1007/s00401-017-1804–9.

[16] X. Hu, B. Das, H. Hou, W. He, R. Yan, BACE1 deletion in the adult mouse reverses preformed amyloid deposition and improves cognitive functions, J. Exp. Med. (2018), https://doi.org/10.1084/jem.20171831.

[17] R. Vassar, P.-H. Kuhn, C. Haass, M.E. Kennedy, L. Rajendran, P.C. Wong, S.F. Lichtenthaler, Function, therapeutic potential and cell biology of BACE proteases: current status and future prospects, J. Neurochem. 130 (2014) 4–28, https://doi.org/10.1111/jnc.12715.

[18] R. Yan, Stepping closer to treating Alzheimer's disease patients with BACE1 inhibitor drugs, Transl. Neurodegener. 5 (2016) 13, , https://doi.org/10.1186/s40035-016-0061-5.

[19] J. Kang, S. Rivest, Lipid metabolism and neuroinflammation in Alzheimer's disease: a role for liver X receptors, Endocr. Rev. 33 (2012) 715–746, https://doi.org/10.1210/er.2011-1049.

[20] M.A. Pappolla, T.K. Bryant-Thomas, D. Herbert, J. Pacheco, M. Fabra Garcia, M. Manjon, X. Girones, T.L. Henry, E. Matsubara, D. Zambon, B. Wolozin, M. Sano, F.F. Cruz-Sanchez, L.J. Thal, S.S. Petanceska, L.M. Refolo, Mild hypercholesterolemia is an early risk factor for the development of Alzheimer amyloid pathology, Neurology. 61 (2003) 199–205.

[21] A. Merched, Y. Xia, S. Visvikis, J.M. Serot, G. Siest, Decreased high-density lipoprotein cholesterol and serum apolipoprotein AI concentrations are highly correlated with the severity of Alzheimer's disease, Neurobiol. Aging 21 (2000) 27–30.

[22] R.W. Mahley, Central nervous system lipoproteins: ApoE and regulation of cholesterol metabolism, Arterioscler. Thromb. Vasc. Biol. 36 (2016) 1305–1315, https://doi.org/10.1161/ATVBAHA.116.307023.

[23] R. Koldamova, N.F. Fitz, I. Lefterov, ATP-binding cassette transporter A1: from metabolism to neurodegeneration, Neurobiol. Dis. 72 Pt A (2014) 13–21, https://doi.org/10.1016/j.nbd.2014.05.007.

[24] W.S. Kim, C.S. Weickert, B. Garner, Role of ATP-binding cassette transporters in brain lipid transport and neurological disease, J. Neurochem. 104 (2008) 1145–1166, https://doi.org/10.1111/j.1471-4159.2007.05099.x.

[25] I. Lefterov, N.F. Fitz, A. Cronican, P. Lefterov, M. Staufenbiel, R. Koldamova, Memory deficits in APP23/Abca1+/− mice correlate with the level of Aβ oligomers, ASN Neuro. 1 (2009), https://doi.org/10.1042/AN20090015.

[26] A. Elali, S. Rivest, The role of ABCB1 and ABCA1 in beta-amyloid clearance at the neurovascular unit in Alzheimer's disease, Front. Physiol. 4 (2013) 45, , https://doi.org/10.3389/fphys.2013.00045.

[27] T. Tokuda, M. Calero, E. Matsubara, R. Vidal, A. Kumar, B. Permanne, B. Zlokovic, J.D. Smith, M.J. Ladu, A. Rostagno, B. Frangione, J. Ghiso, Lipidation of apolipoprotein E influences its isoform-specific interaction with Alzheimer's amyloid beta peptides, Biochem. J. 348 (Pt 2) (2000) 359–365.

[28] D.L. Sparks, S.W. Scheff, J.C. Hunsaker, H. Liu, T. Landers, D.R. Gross, Induction of Alzheimer-like beta-amyloid immunoreactivity in the brains of rabbits with dietary cholesterol, Exp. Neurol. 126 (1994) 88–94, https://doi.org/10.1006/exnr.1994.1044.

[29] C. Cheignon, M. Tomas, D. Bonnefont-Rousselot, P. Faller, C. Hureau, F. Collin, Oxidative stress and the amyloid beta peptide in Alzheimer's disease, Redox Biol. 14 (2017) 450–464, https://doi.org/10.1016/j.redox.2017.10.014.

[30] C. Ghosh, R.M. Dick, S.F. Ali, Iron/ascorbate-induced lipid peroxidation changes membrane fluidity and muscarinic cholinergic receptor binding in rat frontal cortex, Neurochem. Int. 23 (1993) 479–484.

[31] M.O.W. Grimm, J. Mett, H.S. Grimm, T. Hartmann, APP function and lipids: a bidirectional link, Front. Mol. Neurosci. 10 (2017) 63, , https://doi.org/10.3389/fnmol.2017.00063.

[32] T. Kurata, K. Miyazaki, M. Kozuki, N. Morimoto, Y. Ohta, Y. Ikeda, K. Abe, Atorvastatin and pitavastatin reduce senile plaques and inflammatory responses in a mouse model of Alzheimer's disease, Neurol. Res. 34 (2012) 601–610, https://doi.org/10.1179/1743132812Y.0000000054.

[33] B. McGuinness, P. Passmore, Can statins prevent or help treat Alzheimer's disease? J. Alzheimers Dis. JAD. 20 (2010) 925–933, https://doi.org/10.3233/JAD-2010-091570.

[34] C. Schweinzer, A. Kober, I. Lang, K. Etschmaier, M. Scholler, A. Kresse, W. Sattler, U. Panzenboeck, Processing of endogenous AβPP in blood-brain barrier endothelial cells is modulated by liver-X receptor agonists and altered cellular cholesterol homeostasis, J. Alzheimers Dis. JAD. 27 (2011) 341–360, https://doi.org/10.3233/JAD-2011-110854.

[35] M. Zandl-Lang, E. Fanaee-Danesh, Y. Sun, N.M. Albrecher, C.C. Gali, I. Čančar, A. Kober, C. Tam-Amersdorfer, A. Stracke, S.M. Storck, A. Saeed, J. Stefulj, C.U. Pietrzik, M.R. Wilson, I. Björkhem, U. Panzenboeck, Regulatory effects of simvastatin and apoJ on APP processing and amyloid-β clearance in blood-brain barrier endothelial cells, Biochim. Biophys. Acta 1863 (2017) 40–60, https://doi.org/10.1016/j.bbalip.2017.09.008.

[36] A.P. Chirackal Manavalan, A. Kober, J. Metso, I. Lang, T. Becker, K. Hasslitzer, M. Zandl, E. Fanaee-Danesh, J.B. Pippal, V. Sachdev, D. Kratky, J. Stefulj, M. Jauhiainen, U. Panzenboeck, Phospholipid transfer protein is expressed in cerebrovascular endothelial cells and involved in high density lipoprotein biogenesis and remodeling at the blood-brain barrier, J. Biol. Chem. 289 (2014) 4683–4698, https://doi.org/10.1074/jbc.M113.499129.

[37] U. Panzenboeck, Z. Balazs, A. Sovic, A. Hrzenjak, S. Levak-Frank, A. Wintersperger, E. Malle, W. Sattler, ABCA1 and scavenger receptor class B, type I, are modulators of reverse sterol transport at an in vitro blood-brain barrier constituted of porcine brain capillary endothelial cells, J. Biol. Chem. 277 (2002) 42781–42789, https://doi.org/10.1074/jbc.M207601200.

[38] A.C. Kober, A.P.C. Manavalan, C. Tam-Amersdorfer, A. Holmér, A. Saeed, E. Fanaee-Danesh, M. Zandl, N.M. Albrecher, I. Björkhem, G.M. Kostner, B. Dahlbäck, U. Panzenboeck, Implications of cerebrovascular ATP-binding cassette transporter G1 (ABCG1) and apolipoprotein M in cholesterol transport at the blood-brain barrier, Biochim. Biophys. Acta 1862 (2017) 573–588, https://doi.org/10.1016/j.bbalip.2017.03.003.

[39] U. Panzenboeck, I. Kratzer, A. Sovic, A. Wintersperger, E. Bernhart, A. Hammer, E. Malle, W. Sattler, Regulatory effects of synthetic liver X receptor- and peroxisome-proliferator activated receptor agonists on sterol transport pathways in polarized cerebrovascular endothelial cells, Int. J. Biochem. Cell Biol. 38 (2006) 1314–1329, https://doi.org/10.1016/j.biocel.2006.01.013.

[40] B.D. Orio, A. Fracassi, M.P. Cerù, S. Moreno, Targeting PPARalpha in Alzheimer's disease, Curr. Alzheimer Res. (2017), https://doi.org/10.2174/

156720501466617050509454 9.
[41] Y. Jia, J.-Y. Kim, H.-J. Jun, S.-J. Kim, J.-H. Lee, M.H. Hoang, K.-Y. Hwang, S.-J. Um, H.I. Chang, S.-J. Lee, The natural carotenoid astaxanthin, a PPAR-α agonist and PPAR-γ antagonist, reduces hepatic lipid accumulation by rewiring the transcriptome in lipid-loaded hepatocytes, Mol. Nutr. Food Res. 56 (2012) 878–888, https://doi.org/10.1002/mnfr.201100798.
[42] S. Biswal, Oxidative stress and astaxanthin: the novel supernutrient carotenoid, Int. J. Health Allied Sci. 3 (2014) 147, https://doi.org/10.4103/2278-344X.138587.
[43] X.-S. Zhang, X. Zhang, Q. Wu, W. Li, C.-X. Wang, G.-B. Xie, X.-M. Zhou, J.-X. Shi, M.-L. Zhou, Astaxanthin offers neuroprotection and reduces neuroinflammation in experimental subarachnoid hemorrhage, J. Surg. Res. 192 (2014) 206–213, https://doi.org/10.1016/j.jss.2014.05.029.
[44] R. Yamagishi, M. Aihara, Neuroprotective effect of astaxanthin against rat retinal ganglion cell death under various stresses that induce apoptosis and necrosis, Mol. Vis. 20 (2014) 1796–1805.
[45] X.-S. Zhang, X. Zhang, M.-L. Zhou, X.-M. Zhou, N. Li, W. Li, Z.-X. Cong, Q. Sun, Z. Zhuang, C.-X. Wang, J.-X. Shi, Amelioration of oxidative stress and protection against early brain injury by astaxanthin after experimental subarachnoid hemorrhage, J. Neurosurg. 121 (2014) 42–54, https://doi.org/10.3171/2014.2.JNS13730.
[46] X.-S. Zhang, X. Zhang, Q. Wu, W. Li, Q.-R. Zhang, C.-X. Wang, X.-M. Zhou, H. Li, J.-X. Shi, M.-L. Zhou, Astaxanthin alleviates early brain injury following subarachnoid hemorrhage in rats: possible involvement of Akt/bad signaling, Mar. Drugs. 12 (2014) 4291–4310, https://doi.org/10.3390/md12084291.
[47] M.M. Al-Amin, H.M. Reza, H.M. Saadi, W. Mahmud, A.A. Ibrahim, M.M. Alam, N. Kabir, A.R.M. Saifullah, S.T. Tropa, A.H.M.R. Quddus, Astaxanthin ameliorates aluminum chloride-induced spatial memory impairment and neuronal oxidative stress in mice, Eur. J. Pharmacol. 777 (2016) 60–69, https://doi.org/10.1016/j.ejphar.2016.02.062.
[48] M.C. Heck, C.E. Wagner, P.H. Shahani, M. MacNeill, A. Grozic, T. Darwaiz, M. Shimabuku, D.G. Deans, N.M. Robinson, S.H. Salama, J.W. Ziller, N. Ma, A. van der Vaart, P.A. Marshall, P.W. Jurutka, Modeling, synthesis, and biological evaluation of potential retinoid X receptor (RXR)-selective agonists: analogues of 4-[1-(3,5,5,8,8-pentamethyl-5,6,7,8-tetrahydro-2-naphthyl)ethynyl]benzoic acid (bexarotene) and 6-(ethyl(5,5,8,8-tetrahydronaphthalen-2-yl)amino)nicotinic acid (NEt-TMN), J. Med. Chem. 59 (2016) 8924–8940, https://doi.org/10.1021/acs.jmedchem.6b00812.
[49] K. Tanita, T. Fujimura, Y. Sato, T. Hidaka, S. Furudate, Y. Kambayashi, A. Tsukada, A. Hashimoto, S. Aiba, Successful treatment of primary cutaneous peripheral T-cell lymphoma presenting acquired ichthyosis with oral bexarotene monotherapy, Case Rep. Oncol. 10 (2017) 328–332, https://doi.org/10.1159/000468981.
[50] S. De Flora, G. Ganchev, M. Iltcheva, S. La Maestra, R.T. Micale, V.E. Steele, R. Balansky, Pharmacological modulation of lung carcinogenesis in smokers: preclinical and clinical evidence, Trends Pharmacol. Sci. 37 (2016) 120–142, https://doi.org/10.1016/j.tips.2015.11.003.
[51] M.-S. Kim, D.Y. Lim, J.-E. Kim, H. Chen, R.A. Lubet, Z. Dong, A.M. Bode, Src is a novel potential off-target of RXR agonists, 9-cis-UAB30 and Targretin, in human breast cancer cells, Mol. Carcinog. 54 (2015) 1596–1604, https://doi.org/10.1002/mc.22232.
[52] K.P. Koster, C. Smith, A.C. Valencia-Olvera, G.R.J. Thatcher, L.M. Tai, M.J. LaDu, Rexinoids as therapeutics for Alzheimer's disease: role of APOE, Curr. Top. Med. Chem. 17 (2017) 708–720.
[53] P.E. Cramer, J.R. Cirrito, D.W. Wesson, C.Y.D. Lee, J.C. Karlo, A.E. Zinn, B.T. Casali, J.L. Restivo, W.D. Goebel, M.J. James, K.R. Brunden, D.A. Wilson, G.E. Landreth, ApoE-directed therapeutics rapidly clear β-amyloid and reverse deficits in AD mouse models, Science. 335 (2012) 1503–1506, https://doi.org/10.1126/science.1217697.
[54] C. Yuan, X. Guo, Q. Zhou, F. Du, W. Jiang, X. Zhou, P. Liu, T. Chi, X. Ji, J. Gao, C. Chen, H. Lang, J. Xu, D. Liu, Y. Yang, S. Qiu, X. Tang, G. Chen, L. Zou, OAB-14, a bexarotene derivative, improves Alzheimer's disease-related pathologies and cognitive impairments by increasing β-amyloid clearance in APP/PS1 mice, Biochim. Biophys. Acta (BBA) - Mol. Basis Dis. (2018), https://doi.org/10.1016/j.bbadis.2018.10.028.
[55] G. Ren, W. Bao, Z. Zeng, W. Zhang, C. Shang, M. Wang, Y. Su, X.-K. Zhang, H. Zhou, Retinoid X receptor alpha nitro-ligand Z-10 and its optimized derivative Z-36 reduce β-amyloid plaques in Alzheimer's disease mouse model, Mol. Pharm. 16 (2019) 480–488, https://doi.org/10.1021/acs.molpharmaceut.8b00096.
[56] K.D. LaClair, K.F. Manaye, D.L. Lee, J.S. Allard, A.V. Savonenko, J.C. Troncoso, P.C. Wong, Treatment with bexarotene, a compound that increases apolipoprotein-E, provides no cognitive benefit in mutant APP/PS1 mice, Mol. Neurodegener. 8 (2013) 18, https://doi.org/10.1186/1750-1326-8-18.
[57] A.R. Price, G. Xu, Z.B. Siemienski, L.A. Smithson, D.R. Borchelt, T.E. Golde, K.M. Felsenstein, Comment on “ApoE-directed therapeutics rapidly clear β-amyloid and reverse deficits in AD mouse models,” Science. 340 (2013) 924-d. doi:https://doi.org/10.1126/science.1234089.
[58] I. Tesseur, A.C. Lo, A. Roberfroid, S. Dietvorst, B. Van Broeck, M. Borgers, H. Gijsen, D. Moechars, M. Mercken, J. Kemp, R. D'Hooge, B. De Strooper, Comment on “ApoE-directed therapeutics rapidly clear β-amyloid and reverse deficits in AD mouse models,” Science. 340 (2013) 924-e. doi:https://doi.org/10.1126/science.1233937.
[59] D. Goti, A. Hammer, H.J. Galla, E. Malle, W. Sattler, Uptake of lipoprotein-associated alpha-tocopherol by primary porcine brain capillary endothelial cells, J. Neurochem. 74 (2000) 1374–1383.
[60] H. Franke, H. Galla, C.T. Beuckmann, Primary cultures of brain microvessel endothelial cells: a valid and flexible model to study drug transport through the blood-brain barrier in vitro, Brain Res. Brain Res. Protoc. 5 (2000) 248–256.
[61] S. Oddo, A. Caccamo, J.D. Shepherd, M.P. Murphy, T.E. Golde, R. Kayed, R. Metherate, M.P. Mattson, Y. Akbari, F.M. LaFerla, Triple-transgenic model of Alzheimer's disease with plaques and tangles: intracellular Abeta and synaptic dysfunction, Neuron. 39 (2003) 409–421.
[62] L.L. Barnes, R.S. Wilson, J.L. Bienias, J.A. Schneider, D.A. Evans, D.A. Bennett, Sex differences in the clinical manifestations of Alzheimer disease pathology, Arch. Gen. Psychiatry 62 (2005) 685–691, https://doi.org/10.1001/archpsyc.62.6.685.
[63] J.C. Carroll, E.R. Rosario, S. Kreimer, A. Villamagna, E. Gentzschein, F.Z. Stanczyk, C.J. Pike, Sex differences in β-amyloid accumulation in 3xTg-AD mice: role of neonatal sex steroid hormone exposure, Brain Res. 1366 (2010) 233–245, https://doi.org/10.1016/j.brainres.2010.10.009.
[64] P.D. Bowman, A.L. Betz, D. Ar, J.S. Wolinsky, J.B. Penney, R.R. Shivers, G.W. Goldstein, Primary culture of capillary endothelium from rat brain, In Vitro. 17 (1981) 353–362.
[65] J.H. Schefe, K.E. Lehmann, I.R. Buschmann, T. Unger, H. Funke-Kaiser, Quantitative real-time RT-PCR data analysis: current concepts and the novel “gene expression's CT difference” formula, J. Mol. Med. Berl. Ger. 84 (2006) 901–910, https://doi.org/10.1007/s00109-006-0097-6.
[66] U.K. Laemmli, Cleavage of structural proteins during the assembly of the head of bacteriophage T4, Nature. 227 (1970) 680–685.
[67] A. Haid, M. Suissa, Immunochemical identification of membrane proteins after sodium dodecyl sulfate-polyacrylamide gel electrophoresis, Methods Enzymol. 96 (1983) 192–205.
[68] G. Marsche, A. Hammer, O. Oskolkova, K.F. Kozarsky, W. Sattler, E. Malle, Hypochlorite-modified high density lipoprotein, a high affinity ligand to scavenger receptor class B, type I, impairs high density lipoprotein-dependent selective lipid uptake and reverse cholesterol transport, J. Biol. Chem. 277 (2002) 32172–32179, https://doi.org/10.1074/jbc.M200503200.
[69] W. Sattler, D. Mohr, R. Stocker, Rapid isolation of lipoproteins and assessment of their peroxidation by high-performance liquid chromatography postcolumn chemiluminescence, Methods Enzymol. 233 (1994) 469–489.
[70] C. Bergt, K. Oettl, W. Keller, F. Andreae, H.J. Leis, E. Malle, W. Sattler, Reagent or myeloperoxidase-generated hypochlorite affects discrete regions in lipid-free and lipid-associated human apolipoprotein A-I, Biochem. J. 346 (Pt 2) (2000) 345–354.
[71] A. Kozina, S. Opresnik, M.S.K. Wong, S. Hallström, W.F. Graier, R. Malli, K. Schröder, K. Schmidt, S. Frank, Oleoyl-lysophosphatidylcholine limits endothelial nitric oxide bioavailability by induction of reactive oxygen species, PLoS One 9 (2014) e113443, , https://doi.org/10.1371/journal.pone.0113443.
[72] B.T. Casali, G.E. Landreth, Aβ extraction from murine brain homogenates, Bio-Protoc. 6 (2016), https://doi.org/10.21769/BioProtoc.1787.
[73] R. Deane, A. Sagare, K. Hamm, M. Parisi, B. LaRue, H. Guo, Z. Wu, D.M. Holtzman, B.V. Zlokovic, IgG-assisted age-dependent clearance of Alzheimer's amyloid beta peptide by the blood-brain barrier neonatal Fc receptor, J. Neurosci. 25 (2005) 11495–11503, https://doi.org/10.1523/JNEUROSCI.3697-05.2005.
[74] R. Deane, Z. Wu, B.V. Zlokovic, RAGE (yin) versus LRP (yang) balance regulates alzheimer amyloid beta-peptide clearance through transport across the blood-brain barrier, Stroke. 35 (2004) 2628–2631, https://doi.org/10.1161/01.STR.0000143452.85382.d1.
[75] C.-A. Wu, M. Tsujita, M. Hayashi, S. Yokoyama, Probucol inactivates ABCA1 in the plasma membrane with respect to its mediation of apolipoprotein binding and high density lipoprotein assembly and to its proteolytic degradation, J. Biol. Chem. 279 (2004) 30168–30174, https://doi.org/10.1074/jbc.M403765200.
[76] S.E. Lesné, M.A. Sherman, M. Grant, M. Kuskowski, J.A. Schneider, D.A. Bennett, K.H. Ashe, Brain amyloid-β oligomers in ageing and Alzheimer's disease, Brain J. Neurol. 136 (2013) 1383–1398, https://doi.org/10.1093/brain/awt062.
[77] A. Musolino, M. Panebianco, E. Zendri, M. Santini, S. Di Nuzzo, A. Ardizzoni, Hypertriglyceridaemia with bexarotene in cutaneous T cell lymphoma: the role of omega-3 fatty acids, Br. J. Haematol. 145 (2009) 84–86, https://doi.org/10.1111/j.1365-2141.2009.07596.x.
[78] M. Tachibana, M. Shinohara, Y. Yamazaki, C.-C. Liu, J. Rogers, G. Bu, T. Kanekiyo, Rescuing effects of RXR agonist bexarotene on aging-related synapse loss depend on neuronal LRP1, Exp. Neurol. 277 (2016) 1–9, https://doi.org/10.1016/j.expneurol.2015.12.003.
[79] J. Lee, Y. Li, C. Li, D. Li, Natural products and body weight control, North Am. J. Med. Sci. 3 (2011) 13–19, https://doi.org/10.4297/najms.2011.313.
[80] M. Manczak, M.J. Calkins, P.H. Reddy, Impaired mitochondrial dynamics and abnormal interaction of amyloid beta with mitochondrial protein Drp1 in neurons from patients with Alzheimer's disease: implications for neuronal damage, Hum. Mol. Genet. 20 (2011) 2495–2509, https://doi.org/10.1093/hmg/ddr139.
[81] G. Leinenga, J. Götz, Scanning ultrasound removes amyloid-β and restores memory in an Alzheimer's disease mouse model, Sci. Transl. Med. 7 (2015) 278ra33, https://doi.org/10.1126/scitranslmed.aaa2512.
[82] Y. Gong, L. Chang, K.L. Viola, P.N. Lacor, M.P. Lambert, C.E. Finch, G.A. Krafft, W.L. Klein, Alzheimer's disease-affected brain: presence of oligomeric A beta ligands (ADDLs) suggests a molecular basis for reversible memory loss, Proc. Natl. Acad. Sci. U. S. A. 100 (2003) 10417–10422, https://doi.org/10.1073/pnas.1834302100.
[83] S. Lesné, M.T. Koh, L. Kotilinek, R. Kayed, C.G. Glabe, A. Yang, M. Gallagher, K.H. Ashe, A specific amyloid-beta protein assembly in the brain impairs memory, Nature. 440 (2006) 352–357, https://doi.org/10.1038/nature04533.
[84] B.T. Casali, E.G. Reed-Geaghan, G.E. Landreth, Nuclear receptor agonist-driven modification of inflammation and amyloid pathology enhances and sustains cognitive improvements in a mouse model of Alzheimer's disease, J. Neuroinflammation 15 (2018) 43, , https://doi.org/10.1186/s12974-018-1091-y.

[85] N.F. Fitz, A.A. Cronican, I. Lefterov, R. Koldamova, Comment on “ApoE-directed therapeutics rapidly clear β-amyloid and reverse deficits in AD mouse models,” Science. 340 (2013) 924–c. doi:https://doi.org/10.1126/science.1235809.
[86] K. Veeraraghavalu, C. Zhang, S. Miller, J.K. Hefendehl, T.W. Rajapaksha, J. Ulrich, M. Jucker, D.M. Holtzman, R.E. Tanzi, R. Vassar, S.S. Sisodia, Comment on “ApoE-directed therapeutics rapidly clear β-amyloid and reverse deficits in AD mouse models,” Science. 340 (2013) 924-f. doi:https://doi.org/10.1126/science.1235505.
[87] A.W. Corona, N. Kodoma, B.T. Casali, G.E. Landreth, ABCA1 is necessary for bexarotene-mediated clearance of soluble amyloid beta from the hippocampus of APP/PS1 mice, J. Neuroimmune Pharmacol. Off. J. Soc. NeuroImmune Pharmacol. 11 (2016) 61–72, https://doi.org/10.1007/s11481-015-9627-8.
[88] A. Mounier, D. Georgiev, K.N. Nam, N.F. Fitz, E.L. Castranio, C.M. Wolfe, A.A. Cronican, J. Schug, I. Lefterov, R. Koldamova, Bexarotene-activated retinoid X receptors regulate neuronal differentiation and dendritic complexity, J. Neurosci. 35 (2015) 11862–11876, https://doi.org/10.1523/JNEUROSCI.1001-15.2015.
[89] C. Bachmeier, D. Beaulieu-Abdelahad, F. Crawford, M. Mullan, D. Paris, Stimulation of the retinoid X receptor facilitates beta-amyloid clearance across the blood-brain barrier, J. Mol. Neurosci. MN. 49 (2013) 270–276, https://doi.org/10.1007/s12031-012-9866-6.
[90] M. Kuntz, P. Candela, J. Saint-Pol, Y. Lamartinière, M.-C. Boucau, E. Sevin, L. Fenart, F. Gosselet, Bexarotene promotes cholesterol efflux and restricts apical-to-basolateral transport of amyloid-β peptides in an in vitro model of the human blood-brain barrier, J. Alzheimers Dis. 48 (2015) 849–862, https://doi.org/10.3233/JAD-150469.
[91] P.R. Manzine, J.M. de França Bram, E.J. Barham, F. de A.C. do Vale, H.S. Selistre-de-Araújo, M.R. Cominetti, S.C. Iost Pavarini, ADAM10 as a biomarker for Alzheimer's disease: a study with Brazilian elderly, Dement. Geriatr. Cogn. Disord. 35 (2013) 58–66, https://doi.org/10.1159/000345983.
[92] Y.-Q. Wang, D.-H. Qu, K. Wang, Therapeutic approaches to Alzheimer's disease through stimulating of non-amyloidogenic processing of amyloid precursor protein, Eur. Rev. Med. Pharmacol. Sci. 20 (2016) 2389–2403.
[93] E. Kojro, G. Gimpl, S. Lammich, W. Marz, F. Fahrenholz, Low cholesterol stimulates the nonamyloidogenic pathway by its effect on the alpha -secretase ADAM 10, Proc. Natl. Acad. Sci. U. S. A. 98 (2001) 5815–5820, https://doi.org/10.1073/pnas.081612998.
[94] M.F.M. Sciacca, C. Tempra, F. Scollo, D. Milardi, C. La Rosa, Amyloid growth and membrane damage: current themes and emerging perspectives from theory and experiments on Aβ and hIAPP, Biochim. Biophys. Acta (2018), https://doi.org/10.1016/j.bbamem.2018.02.022.
[95] K.S. Vetrivel, G. Thinakaran, Membrane rafts in Alzheimer's disease beta-amyloid production, Biochim. Biophys. Acta 1801 (2010) 860–867, https://doi.org/10.1016/j.bbalip.2010.03.007.
[96] E.P. de Chaves, V. Narayanaswami, Apolipoprotein E and cholesterol in aging and disease in the brain, Future Lipidol. 3 (2008) 505–530.
[97] W.S. Kim, A.S. Rahmanto, A. Kamili, K.-A. Rye, G.J. Guillemin, I.C. Gelissen, W. Jessup, A.F. Hill, B. Garner, Role of ABCG1 and ABCA1 in regulation of neuronal cholesterol efflux to apolipoprotein E discs and suppression of amyloid-beta peptide generation, J. Biol. Chem. 282 (2007) 2851–2861, https://doi.org/10.1074/jbc.M607831200.
[98] L.M. Tai, K.P. Koster, J. Luo, S.H. Lee, Y. Wang, N.C. Collins, M. Ben Aissa, G.R.J. Thatcher, M.J. LaDu, Amyloid-β pathology and APOE genotype modulate retinoid X receptor agonist activity in vivo, J. Biol. Chem. 289 (2014) 30538–30555, https://doi.org/10.1074/jbc.M114.600833.
[99] S. Tamamizu-Kato, J.K. Cohen, C.B. Drake, M.G. Kosaraju, J. Drury, V. Narayanaswami, Interaction with amyloid beta peptide compromises the lipid binding function of apolipoprotein E, Biochemistry. 47 (2008) 5225–5234, https://doi.org/10.1021/bi702097s.
[100] S.E. Wahrle, H. Jiang, M. Parsadanian, J. Kim, A. Li, A. Knoten, S. Jain, V. Hirsch-Reinshagen, C.L. Wellington, K.R. Bales, S.M. Paul, D.M. Holtzman, Overexpression of ABCA1 reduces amyloid deposition in the PDAPP mouse model of Alzheimer disease, J. Clin. Invest. 118 (2008) 671–682, https://doi.org/10.1172/JCI33622.
[101] S.E. Wahrle, H. Jiang, M. Parsadanian, R.E. Hartman, K.R. Bales, S.M. Paul, D.M. Holtzman, Deletion of Abca1 increases Abeta deposition in the PDAPP transgenic mouse model of Alzheimer disease, J. Biol. Chem. 280 (2005) 43236–43242, https://doi.org/10.1074/jbc.M508780200.
[102] M. Iizuka, M. Ayaori, H. Uto-Kondo, E. Yakushiji, S. Takiguchi, K. Nakaya, T. Hisada, M. Sasaki, T. Komatsu, M. Yogo, Y. Kishimoto, K. Kondo, K. Ikewaki, Astaxanthin enhances ATP-binding cassette transporter A1/G1 expressions and cholesterol efflux from macrophages, J. Nutr. Sci. Vitaminol. (Tokyo) 58 (2012) 96–104.
[103] P. Kidd, Astaxanthin, cell membrane nutrient with diverse clinical benefits and anti-aging potential, Altern. Med. Rev. J. Clin. Ther. 16 (2011) 355–364.
[104] H. Yoshida, H. Yanai, K. Ito, Y. Tomono, T. Koikeda, H. Tsukahara, N. Tada, Administration of natural astaxanthin increases serum HDL-cholesterol and adiponectin in subjects with mild hyperlipidemia, Atherosclerosis. 209 (2010) 520–523, https://doi.org/10.1016/j.atherosclerosis.2009.10.012.
[105] O.F. Olesen, L. Dagø, High density lipoprotein inhibits assembly of amyloid beta-peptides into fibrils, Biochem. Biophys. Res. Commun. 270 (2000) 62–66, https://doi.org/10.1006/bbrc.2000.2372.
[106] M. Shinohara, M. Tachibana, T. Kanekiyo, G. Bu, Role of LRP1 in the pathogenesis of Alzheimer's disease: evidence from clinical and preclinical studies, J. Lipid Res. 58 (2017) 1267–1281, https://doi.org/10.1194/jlr.R075796.
[107] S.E. Storck, C.U. Pietrzik, Endothelial LRP1 - a potential target for the treatment of Alzheimer's disease : theme: drug discovery, development and delivery in Alzheimer's diseasege, Pharm. Res. (2017), https://doi.org/10.1007/s11095-017-2267-3.
[108] R. Deane, Z. Wu, A. Sagare, J. Davis, S. Du Yan, K. Hamm, F. Xu, M. Parisi, B. LaRue, H.W. Hu, P. Spijkers, H. Guo, X. Song, P.J. Lenting, W.E. Van Nostrand, B.V. Zlokovic, LRP/amyloid beta-peptide interaction mediates differential brain efflux of Abeta isoforms, Neuron. 43 (2004) 333–344, https://doi.org/10.1016/j.neuron.2004.07.017.
[109] Y. Li, D. Cheng, R. Cheng, X. Zhu, T. Wan, J. Liu, R. Zhang, Mechanisms of U87 astrocytoma cell uptake and trafficking of monomeric versus protofibril Alzheimer's disease amyloid-β proteins, PLoS One 9 (2014) e99939, , https://doi.org/10.1371/journal.pone.0099939.
[110] X. Wen, L. Xiao, Z. Zhong, L. Wang, Z. Li, X. Pan, Z. Liu, Astaxanthin acts via LRP-1 to inhibit inflammation and reverse lipopolysaccharide-induced M1/M2 polarization of microglial cells, Oncotarget. 8 (2017) 69370–69385, https://doi.org/10.18632/oncotarget.20628.
[111] N. Ruderisch, D. Schlatter, A. Kuglstatter, W. Guba, S. Huber, C. Cusulin, J. Benz, A.C. Rufer, J. Hoernschemeyer, C. Schweitzer, T. Bülau, A. Gärtner, E. Hoffmann, J. Niewoehner, C. Patsch, K. Baumann, H. Loetscher, E. Kitas, P.-O. Freskgård, Potent and selective BACE-1 peptide inhibitors lower brain Aβ levels mediated by brain shuttle transport, EBioMedicine. 24 (2017) 76–92, https://doi.org/10.1016/j.ebiom.2017.09.004.
[112] X.-J. Zhao, D.-M. Gong, Y.-R. Jiang, D. Guo, Y. Zhu, Y.-C. Deng, Multipotent AChE and BACE-1 inhibitors for the treatment of Alzheimer's disease: design, synthesis and bio-analysis of 7-amino-1,4-dihydro-2H-isoquilin-3-one derivates, Eur. J. Med. Chem. 138 (2017) 738–747, https://doi.org/10.1016/j.ejmech.2017.07.006.
[113] H.D.Q. Pham, N.Q. Thai, Z. Bednarikova, H.Q. Linh, Z. Gazova, M.S. Li, Bexarotene cannot reduce amyloid beta plaques through inhibition of production of amyloid beta peptides: in silico and in vitro study, Phys. Chem. Chem. Phys. PCCP. 20 (2018) 24329–24338, https://doi.org/10.1039/c8cp00049b.
[114] M. Malnar, M. Kosicek, A. Lisica, M. Posavec, A. Krolo, J. Njavro, D. Omerbasic, S. Tahirovic, S. Hecimovic, Cholesterol-depletion corrects APP and BACE1 misstrafficking in NPC1-deficient cells, Biochim. Biophys. Acta 1822 (2012) 1270–1283, https://doi.org/10.1016/j.bbadis.2012.04.002.
[115] J.L. Cummings, K. Zhong, J.W. Kinney, C. Heaney, J. Moll-Tudla, A. Joshi, M. Pontecorvo, M. Devous, A. Tang, J. Bena, Double-blind, placebo-controlled, proof-of-concept trial of bexarotene in moderate Alzheimer's disease, Alzheimers Res. Ther. 8 (2016) 4, , https://doi.org/10.1186/s13195-016-0173-2.